Seasonal cryogenic processes control supra-permafrost pore water chemistry in two contrasting Cryosols

Julien Fouché, Camille Bouchez, Catherine Keller, Michel Allard, J. P. Ambrosi

Seasonal cryogenic processes control supra-permafrost pore water chemistry in two contrasting Cryosols

Julien Fouché [1], Camille Bouchez [2], Catherine Keller [3], Michel Allard [4], Jean Paul Ambrosi [3]
[1] LISAH, Univ Montpellier, INRAE, IRD, Institut Agro, Montpellier, France
[2] Univ Rennes, CNRS, Géosciences Rennes, UMR 6118, 35000 Rennes, France
[3] Aix Marseille Univ (AMU), CNRS, IRD, INRAE, Coll France, Centre Européen de Recherche et d'Enseignement en Géosciences de l'Environnement (CEREGE), Aix-en-Provence, France
[4] Centre d'Études Nordiques, Université Laval, pav. Abitibi-Price, Québec, Qc, Canada G1K 7P4.

Corresponding author: Julien Fouché
Tel: +0(33) 6 88 70 80 89
Email address: julien.fouche@supagro.fr

Abstract

Over the last decades, Arctic landscapes have experienced intense warming leading to permafrost degradation and rapid ecosystem changes. Active layer thickening, widespread melting of ground ice and thermo-erosion have affected the mobilization of organic and mineral elements. While the carbon and nitrogen cycles are intensively studied, the soil weathering has been less documented. In the present study, we monitored the chemistry of soil capillary and gravitational pore waters, rainfall and stream waters daily during the growing season in two experimental sites under tussock tundra vegetation in the low-Arctic region, in Salluit (Nunavik, Canada). We aimed to investigate the seasonal thaw controls on the evolution of concentrations of major organic and inorganic elements in the active layer (i.e., seasonally thawed surface layers) of two permafrost soils (Cryosols) differing in parental materials: an ombrotrophic bog (i.e., Histic Cryosol) and post-glacial marine sediments continuously waterlogged (i.e., Turbic Cryosol). In the Histic Cryosol, the electrical conductivity was less than 100 µS cm^{-1} and Cl^- and Na^+ were the dominant soluble ions originating from atmospheric depositions. In the Turbic Cryosol, decarbonated in the first 40 cm, Ca^{2+} and Mg^{2+} were the dominant soluble ions in the capillary water reflecting the dissolution of soil minerals, while Cl^- and SO_4^{2-} dominated in gravitational water, illustrating inputs from uphill. In the two soils, Ca^{2+} and Mg^{2+} concentrations as well as Mg/Na and Ca/Na increased with depth. Along summer, the soil pore water chemistry evolved with thaw front and water table depths in the two sites. Particularly in the Histic Cryosol, electrical conductivity, solute concentrations, Mg/Na and Ca/Na ratios increased with the thaw front deepening. Our observations suggest that the active layer thickening and increasing supra-permafrost flow contribution, expected to increase with Arctic warming, could lead to a shift in chemistry of pore waters in organic and mineral permafrost soils, differently depending on permafrost landform settings.

Keywords: Tundra, Soil solution chemistry, Arctic permafrost, Active layer, Lysimeters, Thaw front deepening

1 Introduction

Circumpolar permafrost soils (i.e., Cryosols) represent 16% of the global soil area and store 1035 ± 150 Pg of organic carbon (C) within the first three meters (Hugelius et al., 2014). Cryosols are developed in both organic and mineral materials in which cryogenic processes such as freeze-thawing cycles, cryoturbation, frost heave, cryogenic sorting, cracking and ice segregation dominate pedogenetic processes (Jones et al., 2010; WRB, 2007). With permafrost aggradation and due to low temperatures and poor drainage, the soil weathering and microbial decomposition of organic matter has been limited since the last deglaciation (Davidson and Janssens, 2006; Lindgren et al., 2018; Ping et al., 2014). Consequently, a large pool of organic C has built up in weakly developed soils (Hugelius et al., 2014; Tarnocai and Bockheim, 2011).

Global permafrost warming (Biskaborn et al., 2019) currently leads to permafrost degradation through the gradual thickening of the active layer (seasonally thawed surface layer) (Romanovsky et al., 2015) and the development of thermokarst landforms (land surface subsidence due to the thawing of ice-rich permafrost and the melting of ground ice) (Kokelj and Jorgenson, 2013; Lafrenière and Lamoureux, 2013). The expected increase in precipitation will likely augment the stream discharge, the supra-permafrost contribution to river discharge amplifying the whole hydrological cycle of Arctic landscapes (Bintanja and Selten, 2014; McClelland et al., 2006; Peterson et al., 2002; Zhang et al., 2013). With permafrost degradation, the large pool of previously frozen soil organic matter (SOM) is exposed to decomposition and mobilization, thereby having the potential to generate greenhouse gas emissions that could fuel further global warming (Keuper et al., 2020; Turetsky et al., 2020, 2019). Warming and degradation of permafrost have been shown to increase solute concentrations in surface water bodies via surface and groundwater flow (Beermann et al., 2017; Fouché et al., 2017b; Frey and McClelland, 2009; Harms et al., 2014; Mann et al., 2015; Wickland et al., 2018b) and release sediments into rivers (Jolivel and Allard, 2013; Kokelj et al., 2013; Lewis et al., 2012a) because of enhanced weathering and element leaching (Drake et al., 2018; Kendrick et al., 2018; Kokelj et al., 2013; Vonk et al., 2019; Zolkos et al., 2018). Climate-driven changes in dissolution and solute mobilization from soils to streams will interplay with the carbon cycling in northern watersheds (Hobbie et al., 2002a; Mack et al., 2004; Tank et al., 2012). The mobilization of organic and inorganic elements will evolve in uncertain pathways depending on permafrost soil formation histories, ages, geology, and climate conditions. Therefore, accounting for the contrasting pedogenetic processes in Cryosols and collecting data from soils to streams are crucial to better anticipate the evolution of biogeochemical cycles of northern ecosystems undergoing rapid changes (Ping et al., 2014; Zolkos et al., 2018)(Bouchard et al., 2020; Ulanowski and Branfireun, 2013).

Within the Cryosol diversity, permafrost affected peatlands (i.e., Organic Cryosols) represent 14% of Cryosols. Turbic Cryosols (i.e., cryoturbated soils) dominate Cryosols developed in mineral parental materials representing 61% of northern Cryosols (ACECSS, 1998; Hugelius et al., 2014). Peatlands can be distinguished depending on their chemistry, their hydrology and the hosted plant communities between bogs (i.e. ombrotrophic peatlands) and fens (i.e. minerotrophic peatlands) (Payette et al., 2001; Vitt, 2006). In bogs, only atmospheric depositions provide water and nutrients. Consequently, bogs are strongly limited in nutrients and display low pH. In fens, the soil water is nutrient-rich, slightly acidic to neutral, originating from rainfall and lateral groundwater inputs, and the SOM is moderately to well decomposed (Vasander and Kettunen, 2006). Turbic

Cryosols are developed in various mineral substrates such as glacial, loess or alluvial or marine deposits (Jones et al., 2010; Tarnocai and Bockheim, 2011).

The water availability in the active layer controls the nutrient availability for vegetation and microorganisms (Chu and Grogan, 2010; Schmidt et al., 2002). The composition of pore water (i.e., both capillary and gravitational) integrates atmospheric deposition, supra-permafrost groundwater chemistry, dissolution equilibrium with mineral phases in the soil porosity, root uptake and exudation as well as the dissolution and decomposition of the plant litter and SOM (Nieminen et al., 2013; Ulanowski and Branfireun, 2013). In Cryosols, water only occurs in the liquid state in the active layer during summer and in taliks (i.e., unfrozen ground surrounded by permafrost) strongly limiting pedogenetic processes (Edwards et al., 2006; French, 2007; Ping et al., 2014; Stutter and Billett, 2003). Successive summer leaching has depleted the active layer in major ions while freezing of solute-rich pore water has enriched the deep horizons that thaw at the decadal timescale (i.e., transient layer) (Lamhonwah et al., 2016; Shur et al., 2005). The major solute concentrations could be ten to one hundred times higher in ice lenses just beneath the permafrost table than in the pore water of the active layer (Lamhonwah et al., 2017) thus creating a pool of solutes awaiting release with active layer thickening under warmer climates (Kokelj et al., 2002; Kokelj and Burn, 2005).

The biogeochemical functioning of Arctic watersheds has been mainly investigated through dissolved major solute concentrations and CO_2, CH_4 emissions in ponds and streams (Bagard et al., 2011; Frey and McClelland, 2009; Guo et al., 2007; Humborg et al., 2002; Petrone et al., 2006; Pokrovsky et al., 2012), limiting our ability to infer the intra-catchment processes responsible for the observed changes. Very few studies focused on pore water composition in Arctic Cryosols (Hobbie et al., 2002b; Kokelj et al., 2002; Kokelj and Burn, 2005; Neff and Hooper, 2002; Prokushkin et al., 2007, 2006, 2005; Shibata et al., 2003), and even less used field lysimeters (Carey, 2003; Elberling and Jakobsen, 2000; MacLean et al., 1999; Raudina et al., 2017; Stutter and Billett, 2003), all consistently showing a major control of permafrost conditions and the nature of soils in water biogeochemistry. While some studies have focused on dissolved organic matter cycling (Prokushkin et al., 2006, 2005; Wickland et al., 2018a, 2007) and inorganic elements (Carey, 2003; Kokelj et al., 2002; Raudina et al., 2017; Reyes and Lougheed, 2015; Shibata et al., 2003) in permafrost soils, none performed a high frequency monitoring of the pore water chemistry along summer, investigating the thaw front deepening control on pore water chemistry. As many studies showed that terrestrial ecosystems and surface waters in the Arctic undergo large temporal variations along the year (Beel et al., 2021; Csank et al., 2019; Fouché et al., 2017b; Hughes-Allen et al., 2021; Treat et al., 2018), investigation of seasonal variations of soil functioning is important to better understand the processes at the intra-catchment scale and at soil-water interfaces, which play an crucial role in biogeochemical cycles (Bouchard et al., 2020; Drake et al., 2015; Kokelj et al., 2020; Mann et al., 2015; Wologo et al., 2021). We assume that seasonal variations in permafrost physical states strongly affect soil processes while this control remains unclear and is current knowledge gap (Bouchard et al., 2020). Both chemical (e.g., dissolution of the mineral phase or release of previously frozen solutes) and biological processes (e.g., roots exudates or microbial activity) evolve from the snow melt and the start of deepening of the thaw front to the relatively warm period when the maximum thaw depth is reached and the following late summer experiencing some rainfall events. A better understanding of seasonal processes in Cryosols will provide insights on intra-catchment processes occurring in permafrost landscapes that affect global cycles.

In the present study, we aim at investigating the seasonal thaw effects on biogeochemical cycles at the soil profile scale, for two contrasted soils, in order to provide local processes that may explain the catchment-integrated effects previously observed. To do so, we aim to 1) capture differences in pore water chemistry in Cryosols displaying contrasting parental materials and formation histories, and 2) assess the controls of pore water chemistry evolution along summer. Consequently, we collected water samples daily using tension-free and tension lysimeters in the surroundings of Salluit, in Nunavik (Northern Québec, Canada) along a complete growing season. We monitored for the first time the intra-seasonal variations of concentrations of organic and inorganic solutes in soil pore water in relation with meteorological data, and temperatures, soil moisture and thickness of the active layer in Histic and Turbic Cryosols. We postulate that although the main differences in pore water chemistry are explained by soil parental materials, the seasonal climate (temperature and precipitation) and seasonal cryogenic processes (i.e., thaw front deepening) affect the soil solution chemistry along the growing season in both sites. Although the present study is restricted to a full summer, we believe it will provide a significant assessment of the local interplay between climate-induced active layer thickening and biogeochemical dynamics. We postulate that our results will help evaluating the catchment vulnerability to biogeochemical changes based on the soil extents.

2 Materials and methods

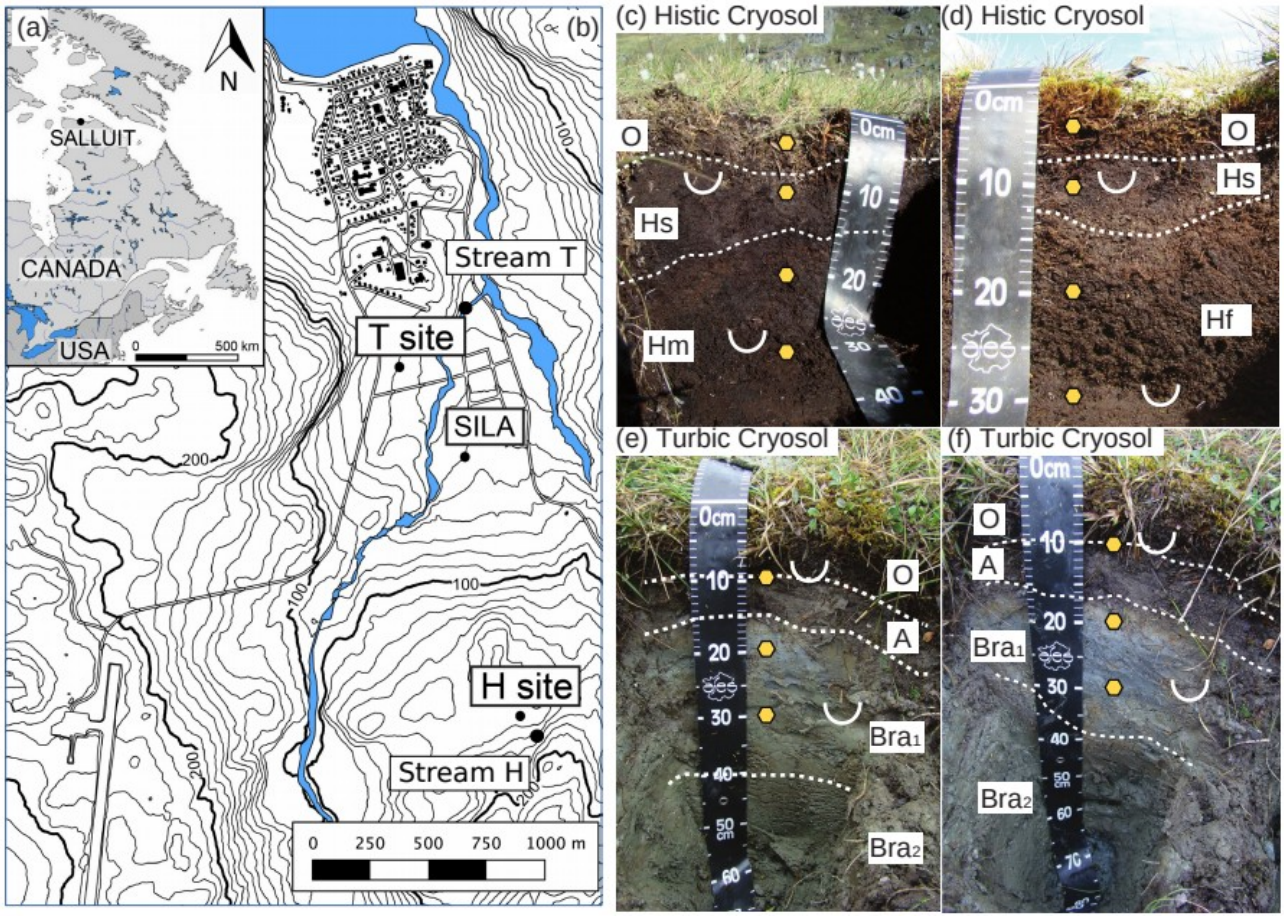

Figure 1: a) Map of the Salluit region and b) locations of the Histic Cryosol and stream at the Histic site (H) and the Turbic Cryosol and stream at the Turbic site (T). Location of the SILA climate station is also shown. Picture of the instrumented soil profiles : Histic Cryosol (c,d) and Reductaquic Turbic Cryosol (e,f). Soil horizons: O, organic layer; Hs, sapric horizon; Hm, hemic horizon; A, organo-mineral horizon; Bra 1,2 , reductaquic horizons (WRB, 2007). The yellow diamonds represent the tension lysimeters, the white semi-circles show the locations of the tension-free lysimeters.

2.1. Study sites and experimental design

The present study focused on two sites situated in Salluit (62°12′N; 75°38′W), lying within the deep continuous permafrost zone on the shore south of Hudson Strait. The permafrost was estimated to be thicker than 150 m under the village near the shore and the active layer thickness locally vary among permafrost landforms (Fouché et al., 2014; Gagnon and Allard, 2020). Measured in many boreholes for more than 30 years, the mean annual ground temperature is -5.6°C at 23 m depth in gneissic bedrock close the airport (Smith et al., 2010). The vegetation is classified as tundra, and mainly composed of tussock-forming sedge (*Eriophorum vaginatum*) and other common herbaceous plants such as Carex bigelowii and Ericaceae *sp.* (Fouché et al., 2014). The two sites differ from their soils: one is a Histic Cryosol (i.e., organic Cryosol) and the other is a Turbic Cryosol reductaquic (Fig 1) (ACECSS, 1998; WRB, 2007). The site characteristics, the experimental design and the environmental monitoring strategy are fully described in Fouché et al. (2014). Briefly, samplings, measurements and analyses were performed at both sites under natural (N) and

warm (W) conditions from early June to early September 2011. The warm conditions were obtained by the installation of open-top chambers, mimicking a temperature increase of ~2°C at the soil surface as used in many tundra warming experiments (Marion et al., 1997). Both the instrument setup and the monitoring procedure were designed to minimize disturbance and to maximize our ability to observe unaltered processes. A meteorological station, from the SILA network of the Centre for Northern Studies (CEN), is located approximately 500 m south of the Turbic site and 1 km north of the Histic site (Fig.1). The mean annual precipitation is 310 mm, of which 52% falls as snow (Kasper and Allard, 2001). The mean annual air temperature monitored in Salluit in 2011 was − 6.3 °C. Mean air and soil surface temperatures recorded at the meteorological station during the measurement period, from June 10 to September 9 2011, were respectively 7.1 °C and 5.1 °C. Rainfalls amounted to 233 mm during the period.

At the Histic site, the two stations were set up in the center of 10 m diameter low center polygons (i.e., slight depression surrounded by elevated rims forming trough above ice wedges). A small stream situated 250 m south and upstream of the H site (further referred to as H stream) drains a small headwater catchment (< 1 km^2) composed of crystalline glacial tills. There is no visible hydrological connection between the Histic Cryosol and the stream (Fig. 1) (Fouché et al., 2014). The Turbic site is located at some elevation on a flat hillside of post glacial marine silts that slopes towards the main stream in Salluit valley, called the Kuuguluk river (Fig. 1). In the back country, the stream watershed is ~10 km^2 wide and is composed of precambrian granites and gneisses of the Churchill Province, till sediments, and deltaic and fine deep-water marine sediments which are associated with the transgression after the last deglaciation and cover the valley floor (Lemieux et al., 2016). In the valley, at low elevations close to the village, the stream flows over marine silts and alluvial and deltaic deposits. The Kuuguluk river will be referred to as T stream in this text.

Two piezometers were installed on either sides of each soil. They were made of perforated and lined PVC pipes, set into 2 m deep drilled holes. Water table depth (WTD) and thaw front depth (TFD, i.e. depth of the interface between unfrozen and frozen soil) were manually measured every day at 3 pm in the piezometers. Over the duration of the project (2010-2011), the active layer thickness averaged at 52 ± 8 cm and 95 ± 5 cm in the Histic and Turbic Cryosols, respectively. The active layer thickness was greater in Turbic Cryosols than in Histic Cryosols due to the low thermal conductivity of dry peat in summer (French, 2007). The volumetric water content of the soil (VWC) was monitored hourly with capacitance sensors EC-5 linked to data loggers Em50 ECHO2 (Decagon Devices, Pullman, WA, USA). Calibrated moisture probes were placed at 10, 20 cm then at 30 cm deep at the Histic site and at 50 cm deep at the Turbic site (Fouché et al., 2017a).

2.2. Soil description

Soils and their properties for each experimental site are presented in Figure 1 and Table 1. The Histic soil is acidic, with a pH around 4.6 throughout the entire profile. The soil organic carbon (SOC) content is constant (~35%) throughout the active layer while the N content slightly increases with depth (from 1.5 to 1.9%). The litter layer of the Histic Cryosol is mainly composed of dead-moss residues which display C/N ratio of 53. The topsoil is a 10 cm thick sapric horizon mainly formed by amorphous organic matter (i.e., highly decomposed organic matter for which plant remains are not discernible) that has a lower porosity than the underlying horizon, which forms the lower part of the active layer. The lower, 15-cm thick, horizon contains between 20 and 50% of

amorphous organic matter and from 50 to 80% of organic matter made of plant tissues. This horizon is slightly different between natural and warm conditions: less plant fibers and more amorphous organic matter provide a denser horizon in the natural condition soil (Hemic horizon = 0.3 g cm^{-3}) than in the warm condition soil (Fibric horizon = 0.2 g cm^{-3}). According to observed hydrological functioning, vegetation communities, and peatland geochemistry, we classified the Histic site as a bog.

The surface organic layer of the Turbic Cryosol, mainly composed of herb residues, is characterized by a pH of 6.5 and a C/N ratio of 26 (Table 1). The 5-cm thick organic layer overlays a 10-cm thick organo-mineral horizon that has a silty clay loam texture (ACECSS, 1998). The lower part of the active layer is composed of two successive mineral reductaquic horizons with thicknesses of 25 cm and 30 cm, respectively. In both natural and warm conditions, the pH is slightly acidic in the first 40 cm (6.3-6.9) and alkaline at the base of the profile (8.1). The cation exchange capacity is around ~30 $cmol^{+}$ kg^{-1} in the topsoil and decreases to ~6 $cmol^{+}$ kg^{-1} in mineral layers at the base of the active layer. The SOC content decreases from ~10% in the topsoil to ~0.5% in the deepest mineral horizon while the N content decreases from 0.8 to ~0.03%.

Mineralogy measurements were performed on a Philips X'PERT PRO X-ray diffractometer with a Cobalt Kα tube with the following settings : 40 mA–40 kV, angle setp of 0.05° and counting times of 4 s, in the Matrix platform at CEREGE (Aix-en-Provence, France). The mineral composition is typical of soils derived from the glacial erosion of surrounded Precambrian metamorphic rocks during the last glaciation. Sometimes considered as “rock flour”, the silty clays are composed of quartz, albite, K-feldspars, chlorite, amphibole (hornblende, riebeckite), illite and muscovite. We found vermiculite in surface horizons and sepiolite and dolomite at the base of the active layer.

Table 1. Soil characteristics in the active layer of the Histic Cryosol (A) and the Turbic Cryosol (B) sampled mi-July 2010.

A) Horizon	**Depth (cm)**	**Texture[a]**	**pH[b]**	**Bulk Density (g cm^{-3})[c]**	**SOC (% DW)[d]**	**STN (% DW)[e]**	**C/N[f]**
Histic Cryosol in natural conditions							
O	0 - 5	-	4.8 ± 0.1	-	41.0 ± 1.8	0.79 ± 0.11	45 ± 4
Sapric horizon	5 - 15	-	4.6 ± 0.0	0.45 ± 0.11	33.1 ± 1.2	1.35 ± 0.14	21 ± 2
Hemic horizon	15 - 25	-	4.6 ± 0.0	0.24 ± 0.03	40.3 ± 1.4	1.88 ± 0.06	18 ± 0
Histic Cryosol in warm conditions							
O	0 - 5	-	4.6 ± 0.0	-	40.6 ± 0.2	0.81 ± 0.08	43 ± 4
Sapric horizon	5 - 12	-	4.6 ± 0.1	0.38 ± 0.08	34.9 ± 1.2	1.66 ± 0.20	18 ± 2
Fibric horizon	12 - 30	-	4.8 ± 0.1	0.19 ± 0.04	35.6 ± 0.7	1.81 ± 0.02	17 ± 1

B) Horizon	**Depth (cm)**	**Texture[a]**	**pH[b]**	**Bulk Density (g cm^{-3})c**	**SOC (% DW)[d]**	**STN (% DW)[e]**	**C/N[f]**	**CEC (cmol^{+} kg^{-1})[g]**	**$CaCO_3$ (g kg^{-1})[h]**	**Olsen P (g kg^{-1})[i]**	**Si (g kg^{-1})[j]**	**Al (g kg^{-1})[j]**	**Fe (g kg^{-1})[j]**
Turbic Cryosol in natural conditions													
O	0 - 5	-	6.5 ± 0.1	-	19.7 ± 1.1	0.82 ± 0.01	21 ± 1	-	-	-	-	-	-
A	5 - 10	Silty clay loam	6.0 ± 0.1	0.55 ± 0.01	13.2 ± 1.4	0.91 ± 0.09	12 ± 1	34.4	<1	0.024	0.064 0.141	0.244 0.212	0.815 1.130
Bra1	10 - 40	Silt loam	6.4 ± 0.2	1.48 ± 0.09	2.1 ± 0.3	0.10 ± 0.01	18 ± 0	6.72	<1	<0.005	0.064 0.111	0.112 0.091	0.509 0.726
Bra2	40 - 70	Silt loam	8.1 ± 0.1	1.49 ± 0.06	0.4 ± 0.4	0.05 ± 0.01	7 ± 1	3.52	26	0.011	0.094 0.151	0.088 0.052	0.405 0.429
Turbic Cryosol in warm conditions													
O	0 - 7	-	6.5 ± 0.1	-	23.7 ± 0.8	0.79 ± 0.02	26 ± 1	-	-	-	-	-	-
A	7 - 15	Silty clay loam	6.6 ± 0.2	1.07 ± 0.06	8.5 ± 0.9	0.54 ± 0.12	14 ± 1	26.7	<1	0.027	0.052 0.144	0.131 0.120	0.448 0.728
Bra1	15 - 40	Silt loam	7.1 ± 0.1	1.56 ± 0.07	1.5 ± 0.2	0.10 ± 0.01	13 ± 0	7.15	<1	<0.005	0.057 0.106	0.113 0.096	0.488 0.757
Bra2	40 - 70	Silt loam	8.1 ± 0.2	1.70 ± 0.02	0.3 ± 0.1	0.03 ± 0.01	9 ± 1	5.34	23	0.015	0.085 0.151	0.092 0.074	0.434 0.626

Mean ± SD calculated from two samplings at all the stations. nd: not determined.
Horizons and their thickness were defined in the field according to the WRB soil classification. Samples were kept cold at 4°C until the end of 2010 when the soil analyses were performed by the INRAE soil laboratory in Arras. Before analyses, soils were oven dried at 40°C and crushed, roots (> 2 mm diameter) were removed by hand and sieved at 2 mm.
[a] The particle size analysis was performed according to the pipet method after organic matter removal (NF X 31-107). Textures were defined thanks to the particle size distributions and according to the US and Canadian Texture Triangle (n = 4).
[b] pH water (n = 4), soil pH was measured after 12h of contact by mixing 10 g of dry soil (oven dry at 40°C) with 50 ml of deionized water.
[c] Bulk density (n = 2), bulk density was measured thanks to undisturbed samples collected with cylinders of 450 cm^3.
[d] Soil organic carbon (SOC) and ([e]) soil total nitrogen (STN) contents were measured by the dry combustion method without decarbonation (NF ISO 10694 and NF ISO 13878). Contents values are expressed in % of the element by dry weight (n = 4).
[f] Atomic ratio between SOC and STN.
[g] Cation exchange capacity (CEC) quantified using Metson method (NF X 31-130). Values are expressed in cmol of positive charges by kg of dry soil (n=1).
[h] Total calcium carbonate content measured by dissolution with HCl (NF ISO 10693). Values are expressed in g by kg of dry soil (n=1).
[i] Inorganic phosphorus extractable with 0.5 M $NaHCO_3$ following Olsen method (NF ISO 11263). Values are expressed in g by kg of dry soil (n=1).
[j] Silicon, aluminum and iron were extracted following Tamm method using oxalic acid (0.0866 mol L^{-1}) and ammonium oxalate (0.1134 mol L^{-1}) at pH 3 and analyzed ICP-AES. The two values refer to the sample analyzed for each station (i.e., N and W) per site.
[K] Mineralogy of bulk soil samples was characterized by X-ray diffraction (XRD) in the Matrix plaform (CEREGE, France) with a X'PERT PRO MPD X-ray diffractometer.

2.3. Stream, rainfall and soil solution sampling and chemical analyses

River water from the H and T streams was sampled once per week from June 24 to September 6, 2011. Rainfall water was sampled from a rain gauge located at the Turbic site from July 1 to September 9 (first snow events occurred mid September, snow was not sampled). Soil pore water samples, including both gravitational and capillary waters, were collected every second day at each site, at different depths from the start of permafrost thawing (i.e. the July 4 at the Histic Site and

June 13 at the Turbic site) to mid-September 2011. Gravitational pore water was sampled from tension-free lysimeters (TFL) placed at 10 and 30 cm deep in the Histic Cryosols (both natural and warm conditions) and Turbic Cryosol in natural conditions, and only 10 cm deep in warm conditions. Capillary pore water was sampled from five tension lysimeters (TL) placed 2, 10, 20, 30, 40 cm deep in the Histic Cryosols and three TL placed 10, 20, 30 cm deep in the Turbic Cryosols. The experimental setup was installed in 2010 and left to stabilize during one year before sampling in 2011. No damage was observed during winter. Tension-free lysimeters collect freely draining water (i.e., gravitational water) in which equilibrium with the soil matrix is not reached while tension lysimeters sample capillary pore water characterized by a longer residence time allowing for equilibrium between water and soil constituents (Nieminen et al., 2013; Parfitt et al., 1997; Watmough et al., 2013). Even though the tension manually applied with a 60 ml syringe for water extraction was not quantified, we estimated it being around 150-500 hPa.

Temperature, EC and pH were measured in soil solutions extracted from TFL. Water samples from TF and TFL were daily filtrated through 0.45 µm GHP Acrodisc glass fibre filters (Pall Corporation, Port Washington, NY, USA) and stored in glass vials for organic analyses and through 0.22 µm Target cellulose acetate filters (National Scientific Company, Rockwood, TN, USA) and stored in polyethylene for inorganic major elements analyses. Before analyses, water samples were kept at ~4°C and later analyzed at the CEREGE laboratory.

Dissolved organic carbon (DOC) contents were measured by high temperature oxidation after inorganic C and volatile C component removal following the NPOC protocol of the TOC-V analyzer (Shimadzu Instruments, Columbia, Maryland, USA). The detection limit of DOC content was ~0.01 mg C L^{-1}. The dissolved total nitrogen (DTN) content was analyzed by the TNM-1 analyzer (Shimadzu Instruments, Columbia, Maryland, USA) with a detection limit of ~0.05 mg N L^{-1}. DOC and TDN were calculated as the mean of three and five injections with the coefficient of variance always <2%. Every run started with milli-Q blanks and with the generation of a new calibration. Analytical errors were estimated from blanks and standard replicates in each run, and reached 7.1% for DOC measurements and 6.9% for TDN measurements. Inorganic anions and cations analyses were performed on a Capillary Ion Analyser (CIA, Waters) with a detection limit of ~0.1 mg L^{-1} for both cations and anions.

2.4. Statistical analysis

All statistical analyses were carried out using the R free software version 3.2.1 (R Core Team, 2012). Bartlett's and Shapiro-Wilk tests were performed to respectively evaluate the variance homogeneity and the normal distribution of each variable. Spearman pairwise correlations between the total solute concentration (TDS), Ca/Na, Mg/Na and Cl/Na ratios, thaw front depth and water table depths were performed to investigate landscape controls on pore water chemistry.
A principal component analysis (PCA), which comprises DOC, DTN, DOC/DTN ratio, TDS, Cl/Na, Mg/Na and Ca/Na ratios, was performed using routines from FactoMineR package. Non-parametric analyses of variance using the multiple pairwise-comparisons using pairwise Wilcoxon rank sum test (defined by its *p value*) were used to determine significant differences in concentrations of solutes and ratios between soil types (Histic vs Turbic) and sampling depths. We chose a threshold of *p values* below *0.001* to define significant differences among groups. Before performing the PCA, auto scaling was conducted on all variables with the FactoMineR package in order to decrease

the leverage of high values. Significance of differences in chemistry composition between soil pore water in natural and warm conditions were tested using PCA results and Wilcoxon rank sum test.

3. Results

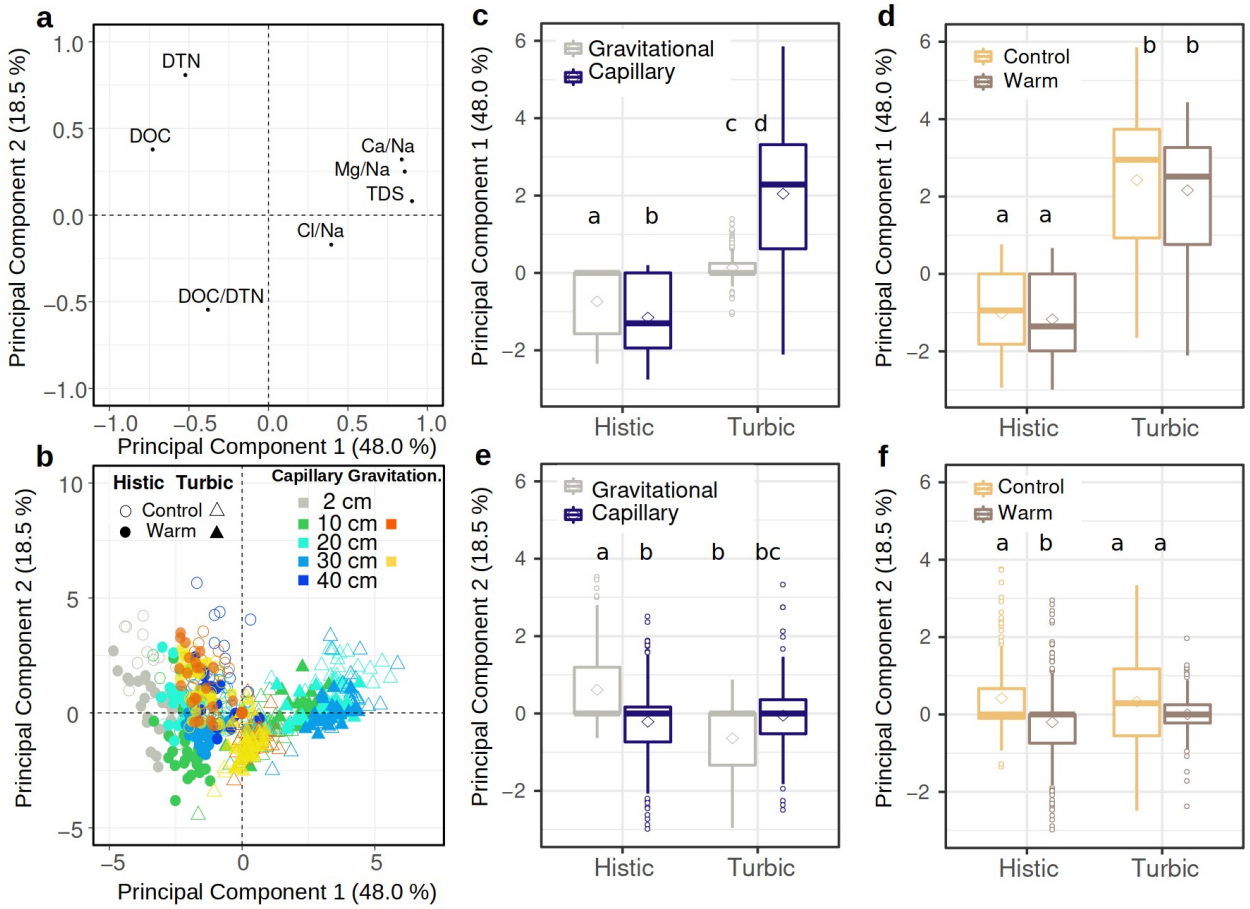

Figure 2: Graphical representations and box plots of the distribution of the scores of the principal component analysis comprising chemistry parameters for rainfall, streams, capillary and gravitational waters in Histic and Turbic Cryosols. a) Loadings of explanatory variables (dissolved organic carbon (DOC, mgC L-1), total dissolved nitrogen (TDN, mgN L-1), DOC/TDN ratio, total dissolved elements (TDS, mol L-1) and major element atomic ratios: Cl/Na, Mg/Na, Ca/Na are shown as black dots. b) Scores across the first and second principal components for samples are presented in capillary and gravitational pore waters (gravitation.) labeled by soil types and depths. Histic samples are shown as circles and Turbic samples as diamonds - and colored by sampling depth and sampling methods. c)d)e)f) Box plots of the distribution of the scores of the two first principal components from the PCA in Histic and Turbic Cryosols in control and warm conditions (c, e), in capillary and gravitational waters (d, f). Letters indicate significant differences between depths, soil types and types of lysimeters, according Wilcoxon rank sum test and difference significance chosen for p-values below 0.001 (i.e., similar letters stand for no significant mean differences, on the contrary different letters represent different means among groups – conditions + sampling methods). In each box plot the diamond represents the mean, the horizontal line represents the median, the end of the box the 25th and 75th percentiles and the lines extending from the box are 1.5 interquartile ranges from the median. Points outside of the interval are presented as dots.

Soil thermal regimes, variations in volumetric water contents, water table and thaw front depths during summer 2011 in both Histic and Turbic Cryosols are presented in Fouché et al. 2017a. Ground thaw occurred in three phases: 1- slow deepening of the thaw front from the beginning of June to mid-July, followed by 2- a quick thawing phase up to early August; 3- since mid-August, the maximum thaw depth was reached being respectively ~ 60 cm in the Histic Cryosol and ~100 cm in the Turbic Cryosol. Once thawed, the volumetric water content of soil horizons remained almost steady, close to saturation, at all depths for both soils during the entire summer (Fouché et al., 2017a).

3.1. Vertical and temporal variations in pore water composition

The chemistry of pore waters collected in Histic and Turbic soils are shown in Table S1 and Table S2. Seasonal trends in pore water chemistry are presented in supplementary materials (Fig. S1, S2, and S3). The multi-variate statistical analyses based on DOC, DTN, DOC/DTN, TDS, and Cl/Na, Mg/Na and Ca/Na ratios was conducted using all samples (i.e., capillary and gravitational pore waters, rainfall and streams waters). The PCA displays two first components accounting for 66.5% of the total variance, and shows a clear separation of water samples both between the soil types and between the capillary and gravitational pore waters independently of sampling depth (Fig. 2a,b,c). The first component of the PCA represents the enrichment in TDS, Ca/Na and Mg/Na ratios on the positive side and the DOC enrichment on the other side (Fig. 2a). The second component of the PCA represents a DTN enrichment and a decrease in DOC/DTN (Fig. 2a). No significant differences were shown between the normal and warm conditions at each site and therefore data are later pooled together to investigate seasonal controls of pore water composition at the site scale (Table S1, S2, Fig. 2c,e).

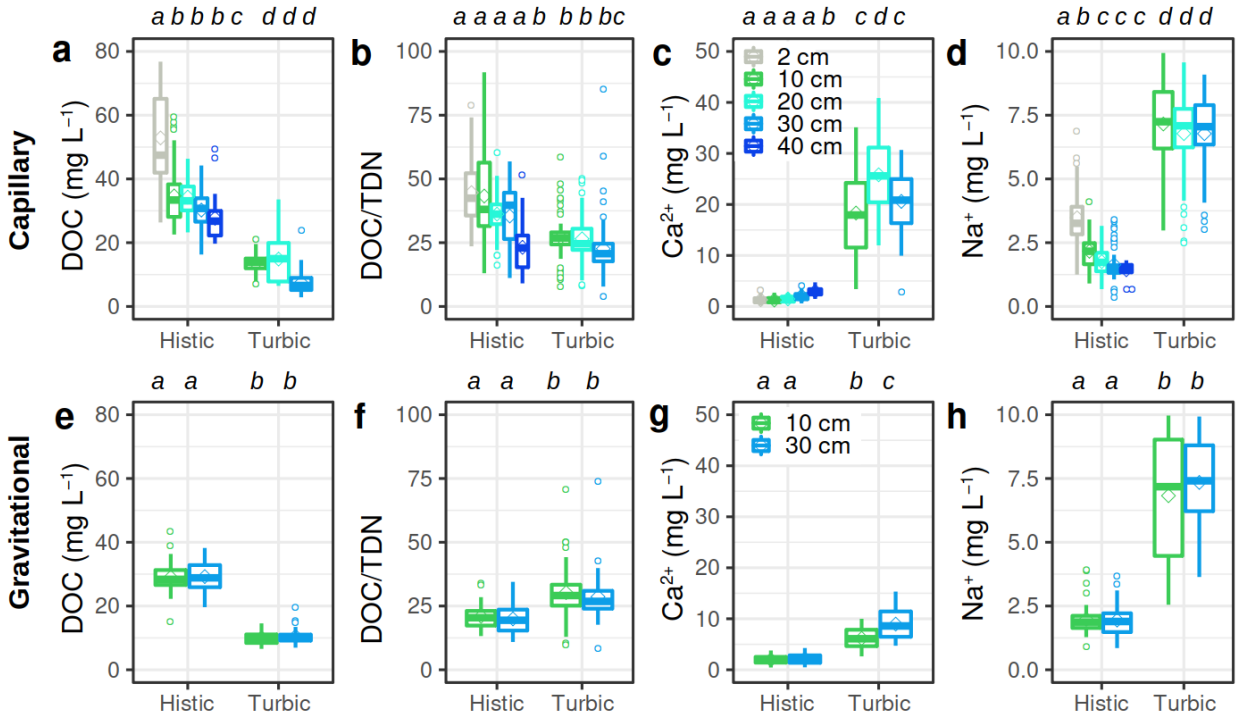

Figure 3: Total dissolved solutes and dissolved organic carbon concentrations and the ratio between dissolved organic carbon and total dissolved nitrogen (DOC/DTN) in the Histic and Turbic Cryosol pore waters. Samples are grouped by depths (2, 10, 20, 30 and 40 cm) and by types of pore water (capillary and gravitational waters). Letters indicate significant differences between depth, soil types and types of lysimeters, according Wilcoxon rank sum test and difference significance chosen for p-values below 0.001 (i.e., similar letters stand for no significant mean differences, on the contrary different letter represent the variable means are different among groups – soil type + sampling depth). The box plots summarize the distribution of a)d) the concentration of total solutes (mol L-1) and b)e) dissolved organic carbon (mg L-1) and c)e) the ratio DOC/DTN for each depth. In each boxplot, the diamond represents the mean, the horizontal line represents the median, the ends of the box the 25th and 75th percentiles respectively and the lines extending from the box are 1.5 interquartile ranges from the median. Points outside of the interval are presented as dots.

3.1.1. Gravitational and capillary pore water composition in the Histic Cryosol

The gravitational water (i.e., sampled with tension-free lysimeters) in the active layer of the Histic Cryosol was slightly acidic at all depths (pH = 5.3 ± 0.6). The EC ranged from 22.2 to 105.0 µS cm^{-1}, increasing along from early July to mid-August and decreasing afterwards (Fig. S1).

Mean DOC contents averaged ~30 mgC L^{-1} in both gravitational and capillary pore waters (i.e., sampled with tension lysimeters) at 10 and 30 cm depths (Fig. 3, Table S1). Mean DTN contents were lower in capillary than in gravitational waters (Table S1). In capillary water, DOC concentrations decreased with depth from ~60 mgC L^{-1} at 2 cm deep to ~20 mgC L^{-1} at 40 cm deep (Table S1, Fig. 3). At 20, 30 and 40 cm deep, DOC and DTN contents in capillary water remained almost steady over the growing season (Fig. S2). The DOC:TDN ratio, which decreased with depth, was lower in gravitational than in capillary waters (Table S1, Fig. 3). In capillary water, DOC/DTN ratio was similar to soil C/N in the corresponding horizons (Table 1 and Table S2).

The major solute concentrations in gravitational water did not differ from concentrations in capillary water at 10 and 30 cm (Table S1, Fig. 3). Both gravitational and capillary pore waters of

the Histic Cryosol displayed low concentrations of major solutes (Table S1) with TDS averaging 8.49 mg L^{-1} (i.e., 0.28 mol L^{-1}). Capillary water at 2 cm and 40 cm deep was significantly more concentrated in solutes than at the 10, 20 and 30 cm deep (Table S1, Fig. 3). In all pore waters, SO_4^{2-}, NO_3^- and K^+ concentrations were below the detection limits (Table S1). Mean Na^+ concentrations were weakly correlated with Cl^- ($r = 0.29$, $p < 0.001$) and decreased with depth (Table S2). Concentrations of Mg^{2+} and Ca^{2+}, which were positively correlated ($r = 0.73$, $p < 0.001$), increased with depth (Table S1, Fig. 3). Mg^{2+} and Ca^{2+} concentrations in both gravitational and capillary waters increased from June to mid-August and decreased afterwards (Fig. S3, Fig. S4).

3.1.2. Gravitational and capillary pore water composition in the Turbic Cryosol

The gravitational water pH was on average 6.8 (Table S2). The EC, which increased with depth, ranged from 103.0 to 424.0 µS cm^{-1} (Fig. S1, Table S2). After a quick increase during June, EC remained steady over July and August and slightly decreased during the end of summer (Fig. S1).

While DOC concentrations were higher in capillary than gravitational waters at 10 cm deep, they were similar at 30 cm deep (Table S2). In contrast, DTN concentrations did not differ between gravitational and capillary waters (~0.4 mgN L^{-1}, Table S2). DOC concentrations did not differ between depths in gravitational water (Fig. 3, Table S2) while they decreased from 10 to 30 cm deep in capillary pore water (Fig. 3). Accounting for all samples, DOC concentrations correlated with TDN ($r = 0.52$, $p < 0.001$). In both gravitational and capillary waters, DOC concentrations showed quick variations during the first weeks then they remained almost steady (Fig. S3). The DOC/DTN ratio was higher than soil C/N in the corresponding horizons but was close to C/N in the O horizons, where SOC and STN were the greatest (Table 1, Table S2). DOC/DTN ratio in capillary water, which decreased with depth, was slightly lower than in gravitational water (Table S2, Fig. 3).

Gravitational water displayed lower major solute concentrations than capillary water, TDS averaging 38.25 ± 11.82 and 67.26 ± 19.39 mg L^{-1}, respectively (Fig. 2, 3, Table S2). Nitrate concentrations were below the detection limit (Table S2). Mean concentrations of Cl^-, SO_4^{2-}, Ca^{2+} and Mg^{2+} showed significant differences between water sampling methods (Table S2). Major anions (Cl^-, SO_4^{2-}) were less concentrated in capillary than in gravitational waters while Ca^{2+} and Mg^{2+} concentrations were higher in capillary pore water (Table S3). Concentrations of K^+ were higher in capillary water at 30 cm deep. In contrast, Na^+ concentrations did not significantly differ between sampling methods (Table S2). In capillary water, Mg^{2+} concentrations were correlated to Ca^{2+} ($r = 0.61$, $p < 0.001$). Concentrations of Na^+, Ca^{2+} and Cl^- were weakly correlated to each other (Ca^{2+} vs Na^+: $r = 0.29$, $p < 0.001$; $Na^+$and Cl^- : $r = 0.34$, $p < 0.001$; $Ca^{2+}$and Cl^- : $r = 0.26$, $p < 0.001$). Mean Cl^- concentrations in capillary waters increased over summer and decreased with depth (Fig. S3). Na^+ concentrations did not evolve with depth, while concentrations of SO_4^{2-}, Ca^{2+}, Mg^{2+} and K^+ increased with depth (Fig. 3, Table S3).

Table 2: Mean chemical composition of rainfall and stream waters.

	Sites	n[a]	T(°C)[b]	pH	EC (µS cm^{-1})[c]	DOC (mgC L^{-1})[d]	DTN (mgN L^{-1})[e]	DOC/DTN
Rainfall		12	/	5.7 ± 0.1	9.7 ± 3.1	1.1 ± 0.5	0.2 ± 0.2	9.1 ± 8.0
Streams	***H***	13	4.6 ± 1.2	6.1 ± 0.6	102.4 ± 25.4	4.8 ± 1.6	0.2 ± 0.0	27.6 ± 15.3
	T	13	9.0 ± 2.9	6.4 ± 1.1	37.7 ± 12.7	3.2 ± 1.2	0.2 ± 0.1	29.4 ± 28.6

	Sites	Cl^- (mg L^{-1})	SO_4^{2-} (mg L^{-1})	NO_3^- (mgN L^{-1})	Ca^{2+} (mg L^{-1})	K^+ (mg L^{-1})	Mg^{2+} (mg L^{-1})	Na^+ (mg L^{-1})
Rainfall		1.1 ± 1.1	0.5 ± 0.5	< 0.1	< 0.1	< 0.1	0.1 ± 0.1	0.5 ± 0.5
Streams	***H***	3.4 ± 1.2	14.8 ± 9.3	< 0.1	2.8 ± 1.0	1.0 ± 0.3	0.7 ± 0.3	1.8 ± 0.4
	T	3.7 ± 1.0	3.8 ± 2.6	< 0.1	0.7 ± 0.2	0.8 ± 0.4	0.8 ± 0.2	1.8 ± 0.5

Mean ± SD calculated from water samples collected during the three months of study.
[a] number of samples (n) analyzed,
[b] temperature (°C), [c] electrical conductivity normalized at 25°C (EC) of soil solution during sampling,
[d]DOC and [e]DTN correspond to dissolved organic carbon and dissolved total nitrogen.

3.2. Geochemistry of rainfall and stream waters

Rainfall waters were acidic (pH = 5.7 ± 0.1) and EC was 9.7 ± 3.1 µS cm^{-1}. Concentrations of DOC and DTN were 1.1 ± 0.5 and 0.2 ± 0.2 mg L^{-1} in rainfall and positively correlated to each other ($r = 0.67$, $P < 0.001$). DOC/DTN ratio averaged 9.1 ± 8.0. No trend over summer was observed (Fig S4). Concentrations of Cl^- and Na^+ were strongly correlated (respectively $r = 0.93$, $p < 0.001$), showing a common origin. Cl^-, SO_4^{2-} and Na^+ were the most concentrated ions in rainfall waters.

The H stream temperature remained almost steady between 2-6 °C while the T stream warmed up until July and cooled down during late summer (Fig S4). Stream waters were slightly acidic (H stream: 6.1 ± 0.6; T stream: 6.4 ± 1.1). The EC, which increased along summer, was higher in the H stream than in the T stream (Fig S4, Table 2). Concentrations of DOC, which were lower in the T stream (3.2 ± 1.2 mg L^{-1}) than in the H stream (4.8 ± 1.6 mg L^{-1}), were not correlated to DTN concentrations and did not display any trends during summer (Fig S4). The DOC/DTN ratio averaged 27.6 ± 15.3 in the H stream and 29.4 ± 28.6 in the T stream. Ca^{2+} and SO_4^{2-} were more concentrated in the H stream than in the T stream (Table 2). The concentrations of Ca^{2+}, Mg^{2+} and SO_4^{2-} increased along summer and NO_3^- were below detection limit in the two streams (Table 2, Fig S4).

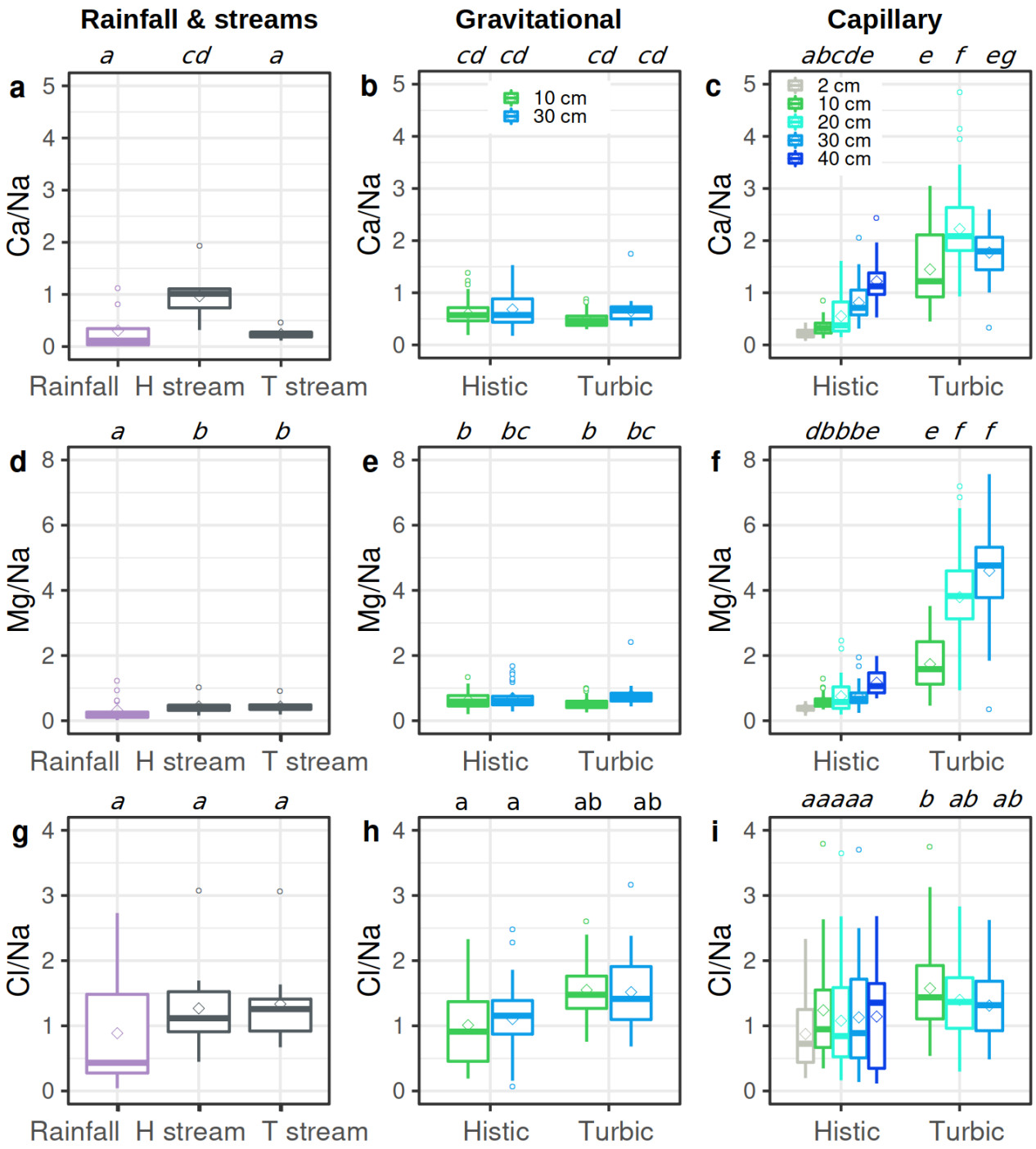

Figure 4: Box plots of atomic elemental ratios of Mg/Na, Ca/Na and Cl/Na in rainfall and stream water, and in the Histic and Turbic Cryosol pore waters. Samples are grouped by depth (2, 10, 20, 30 and 40 cm) and by type of pore water (capillary and gravitational waters). The box plots summarize the distribution of a)b,c) Ca/Na and d,e,f) Mg/Na and g,h,i) Cl/Na for rainfall, stream waters and at each sample depth in studied Cryosols. Letters indicate significant differences differences between rainfall, streams, depths, soil and pore water types according Wilcoxon rank sum test and difference significance chosen for p-values below 0.001 (i.e., similar letters stand for no significant mean differences, on the contrary different letter represent different means among groups – soil type + sampling depth). In each box plot the diamond represents the mean, the horizontal line represents the median, the end of the box the 25th and 75th percentiles and the lines extending from the box are 1.5 interquartile ranges from the median. Points outside of the interval are presented as dots.

3.3. Differences in composition of Cryosol pore waters and surface waters

Capillary and gravitational waters of Turbic Cryosols were more concentrated in major inorganic solutes but less concentrated in DOC and TDN than Histic Cryosols waters (Fig. 3, Table S1, S2). DOC/DTN ratios of soil pore waters, which were slightly higher in the Histic than Turbic Cryosol, were higher than values in rainfall waters and close to values found in stream waters. In the Histic Cryosols, both capillary and gravitational waters displayed higher concentrations in DOC, DTN and lower concentrations in SO_4^{2-} than the H stream water (Table 2, Table S1, S2). In Turbic Cryosols, the capillary water was more concentrated in solutes than rainfall water and the T stream water while gravitational water displayed similar solute concentrations as rainfall and the T stream water (Table 2, Table S1, S2).

Mg/Na and Ca/Na ratios are positively correlated in both stream and soil pore waters (Fig. S5). However, Mg/Na and Ca/Na ratios differed between rivers and pore waters, and among the different sampling depths (Fig. 4). In gravitational pore water, Mg/Na, Ca/Na and Cl/Na ratios were similar between Turbic and Histic Cryosols. Turbic Cryosol capillary pore water displayed higher Mg/Na and Ca/Na ratios than Histic Cryosol capillary water (Fig. 4). In the Turbic Cryosol, ratios were higher in capillary than in gravitational waters (Fig. 4). In the Histic Cryosol, Mg/Na and Ca/Na ratios were similar between capillary and gravitational waters at similar depth (Fig. 4). Cl/Na ratio was similar in rainfall, stream waters and capillary and gravitational waters from both soils (Fig. 4). In both Cryosols, Ca/Na and Mg/Na ratios of capillary water increased with depth while Cl/Na did not (Fig. 4).

In the Histic Cryosol, Ca/Na ratio was similar in gravitational waters, capillary pore waters at 20 and 30 cm deep and in the H stream water. Capillary waters at 2 cm and 10 cm displayed lower Ca/Na ratios than deeper in the soil profile as the surface layer displayed similar Ca/Na ratio as rainfall (Fig. 4). Ca/Na ratio was the highest at 40 cm deep. In the Histic Cryosol, gravitational and capillary waters from 2 to 20 cm depths displayed similar Mg/Na ratio as the H stream and higher than rainfall. Mg/Navalues were higher at 30 and 40 cm deep in capillary water than H stream (Fig. 4, Fig. S5). In the Histic Cryosol, the composition of capillary water at 30 and 40 cm depth were closer to the stream water composition than capillary water from surface layers (Fig. 4).

In the Turbic Cryosol, Mg/Na and Ca/Na ratios in capillary and gravitational waters were higher than rainfall and T stream waters (Fig. 4, Fig. S5). Turbic Cryosol capillary waters displayed an enrichment in Mg^{2+} compare to Ca^{2+} with depth (Fig. 4).

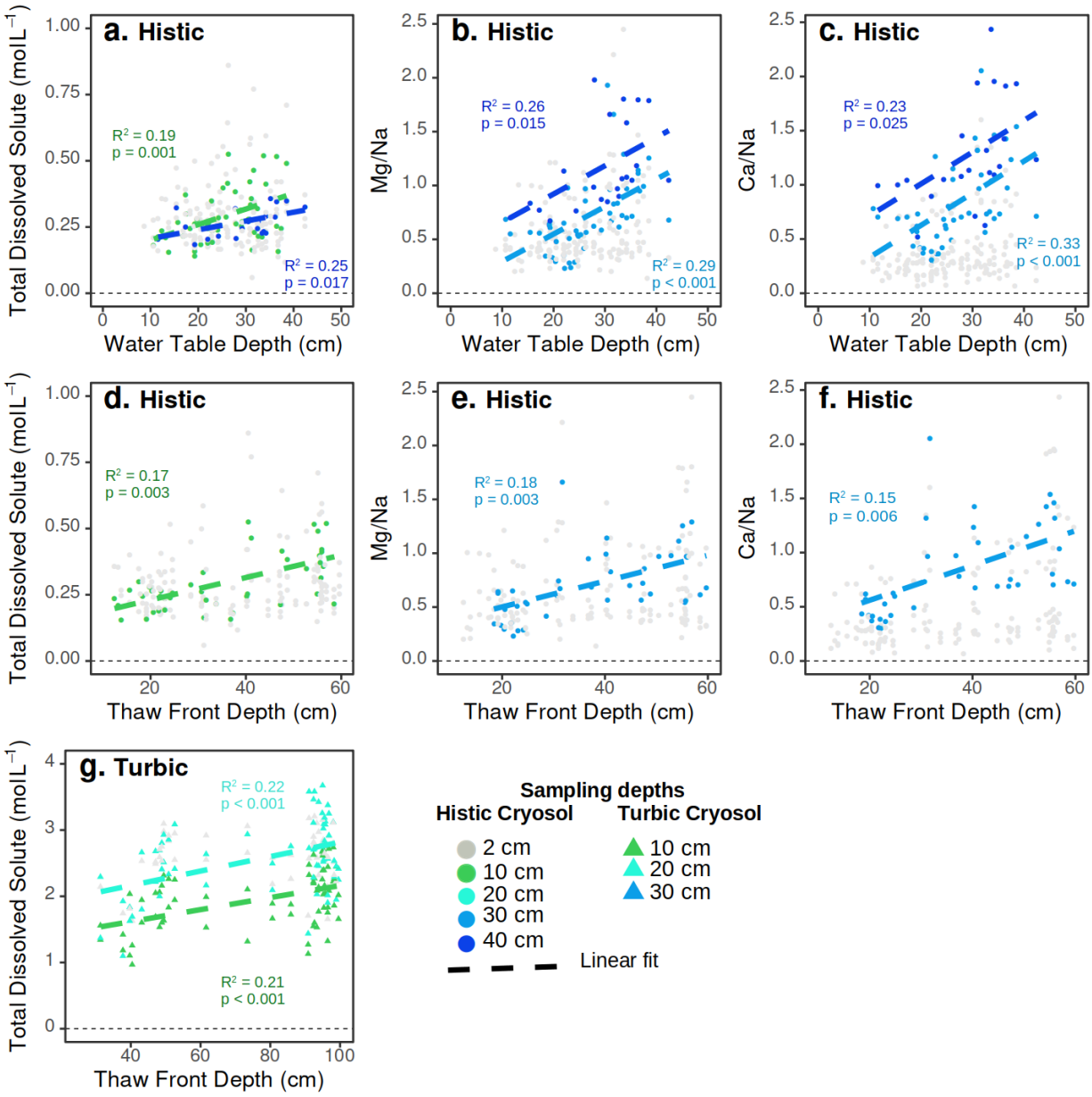

Figure 5: Relationships between total dissolved solutes, Mg/Na and Ca/Na atomic ratios, and the water table and the thaw front depths during summer for capillary pore water. a)b)c) Chemistry parameters plotted against the water table depth in the Histic Cryosol. d)e)f) Chemistry parameters plotted against the thaw front depth in the Histic Cryosol. g) Total dissolved solutes plotted against the thaw front depth in the Turbic Cryosols. Each point represents one sample labeled by Cryosol (Histic or Turbic) and depths. Only the significant relationships between chemistry and water table or thaw front depth ($p < 0.05$) are colored. The Spearman correlation coefficients associated with the regression lines (dashed lines) are shown in Table S3 and Table S4. All samples are shown in Fig S6 and Fig S7. Natural and warm condition samples are combined.

3.4. Evolution of pore water composition with thaw front and water table depths

Volumetric water contents at the different sampling depths were almost constant over summer (Fouché et al., 2017a), therefore water contents likely did not play a key role in pore water chemistry. As thaw front deepening integrates seasonal temperature changes, we focused our investigation of landscape controls on pore water chemistry on thaw front and water table depth.

In the Histic Cryosol capillary waters, TDS increased with thaw front deepening at 10 cm (Fig. 5, Fig. S6; Table S3). In gravitational water at 10 cm and capillary water at 30 cm deep, Ca/Na, Mg/Na and Cl/Na ratios increased with thaw front depth (Fig. S6; Table S3). In the Turbic Cryosol, concentrations of TDS increased with thaw front depth in capillary and gravitational waters at 10 and 20 cm deep (Fig. 5, Fig. S6; Table S3). In Turbic Cryosol gravitational water, Ca/Na and Mg/Na decreased with thaw front depth illustrating a relative enrichment in Na in surface layers with thaw front deepening. No relationships were observed between thaw front depth and elemental ratios in the capillary waters in the Turbic Cryosols. In gravitational water of both soils, EC increased with thaw front depth but did not evolve with water table depth (Fig. S7).

In the Histic Cryosol, Mg/Na and Ca/Na ratios increased with water table depth in capillary pore water from 10 to 40 cm depth (Fig. 5, Fig. S8, Table S4) meaning deeper was the saturated zone, more enriched in Mg and Ca were capillary waters in the soil profile. Cl/Na ratio increased with water table deepening in capillary waters of surface layers (Table S4) illustrating a relative enrichment in Cl in surface layers with a deeper saturated zone. In the Turbic Cryosol, while TDS did not evolve with water table depth, Mg/Na, Ca/Na and Cl/Na increased with water table deepening in gravitational water at 10 cm deep (Fig. 5, Fig. S8, Table S4).

4. Discussion

4.1. Water sources and chemistry from rainfall to soils and streams

Upon permafrost degradation, a portion of the permafrost organic and mineral pools is mobilized and processed from soils to surface waters. A better characterization the water chemistry in permafrost landscapes will allow for understanding intra-catchment processes that affect global cycles. The geochemistry of sampled rainfall water was dominated by Cl^-, SO_4^{2-} and Na^+ illustrating the contribution of sea sprays from coastal wet and dry deposition. Rainfall pH was slightly higher than reported values in Arctic ecosystems ranging from 4.0 to 5.0 (Darmody et al., 2000; Reimann et al., 1997). In contrast, measured EC values in rainfall were lower than published values in coastal regions (from ~13 to ~164 µS cm^{-1}) (Santos et al., 2011; Vazquez et al., 2003) but were similar to rainfall waters reported in the Arctic in Darmody et al. (2000). Values of pH and EC in rainfall were also consistent with reported values from Arctic surface snow, which ranged from 5.1 to 6.0 and from 3.9 to 14.8 µS cm^{-1}, respectively (Darmody et al., 2000; de Caritat et al., 2005; Douglas and Sturm, 2004; Krnavek et al., 2012). As expected in tundra environments, the rainfall DOC values of the present study were low (~1 mg L^{-1}) and were consistent with values in wet deposition reported globally (Iavorivska et al., 2016) and in northern ecosystems (Pan et al., 2010; Willey et al., 2000).

Despite the great diversity of formation histories, geology, sizes, and climate conditions of Arctic watersheds, the chemistry of the studied streams is consistent with previous studies investigating Arctic rivers (Fouché et al., 2017b; Lewis et al., 2012b; McNamara et al., 2008; Zarnetske et al., 2007). Both streams showed DOC and TDN concentrations within the low limits of reported

values in similar contexts, reported values of DOC concentrations ranging from ~2 to ~21 mg L^{-1} (Bagard et al., 2011; Fouché et al., 2017b; Humborg et al., 2002; Lewis et al., 2012b; Mann et al., 2015; Pastor et al., 2020; Pokrovsky et al., 2006; Spencer et al., 2009; Wickland et al., 2012). The two studied streams drained waters poorly concentrated in major solutes (Avagyan et al., 2016; Bagard et al., 2011; Darmody et al., 2000; Fouché et al., 2017b; Humborg et al., 2002; Lamhonwah et al., 2017; Lewis et al., 2012b; Pokrovsky et al., 2006, 2005; Zolkos et al., 2018), . The low concentrations suggest a short water transfer time and a limited weathering occurring in the catchment.

The low atomic Mg/Na (0.1-1.0), Ca:/Na (0.1-2) ratios found in rivers are close to the sea water ratios (Ca/Na and Mg/Na ratios of ~0.1) but reveal small weathering of silicates, as the silicate end member is characterized by Ca:Na = 0.35 ± 0.15 and Mg/Na = 0.24 ± 0.12 (Gaillardet et al., 1999; Picouet et al., 2002). Silicate weathering is consistent with the dominance of crystalline bedrock and silicate-rich till in both stream catchments (Brennan et al., 2014; Lemieux et al., 2016; Négrel et al., 1993; Picouet et al., 2002; Viers et al., 2000)

Along summer, streams showed an increase in EC, and in concentrations of SO_4^{2-}, Mg^{2+} and Ca^{2+} as reported in many headwater streams in the Arctic (Fouché et al., 2017b; Frey and McClelland, 2009; Keller et al., 2010; Lamhonwah et al., 2017; Lewis et al., 2012b; Petrone et al., 2006). It is interpreted as the mobilization and export of ions from the solute-rich horizons at the base of the active layer by supra-permafrost groundwater flows (Lamhonwah et al., 2017). The deepening of the active layer during summer increases the contribution of supra-permafrost groundwater to river discharge (Sjöberg et al., 2021), which transports higher dissolved solute loads.

Different soil solution fractions, characterized by water various residence times in the porosity, are sampled by the tension-free and tension lysimeters. Although some studies highlighted concentration differences between gravitational and capillary waters, no general trend has been found yet (Nieminen et al., 2013; Parfitt et al., 1997; Watmough et al., 2013). In Histic Cryosols, longer residence time does not affect the major element concentrations as the soil matrix is organic, which rather depend on the mixing between two water sources: atmospheric deposition and solute-rich groundwater inputs (Hribljan et al., 2018; Ulanowski and Branfireun, 2013).

4.2. Pore water chemistry in the Histic Cryosol reflects landscape processes

Soil properties of the Histic Cryosol were similar to boreal and tundra organic Cryosols (Hodgkins et al., 2014; Schädel et al., 2014; Wickland et al., 2018a). The Histic Cryosol exhibits a low pH consistent with its ombrotrophic functioning and a great content of organic acids released by the peatland vegetation and organic matter decomposition. The pore water chemistry was similar to values reported in permafrost peatlands in various permafrost environments (Avagyan et al., 2016, 2014; Beer et al., 2008; Jessen et al., 2014; O'Donnell et al., 2016; Raudina et al., 2021, 2018, 2017; Ulanowski and Branfireun, 2013; Wickland et al., 2018a, 2007; Zhang et al., 2017). To our knowledge, no TDN concentration in pore water sampled with the same methods exist for similar environments.

As expected, both gravitational and capillary waters in histic horizons were enriched in DOC and DTN and depleted in major elements compare to mineral Cryosols, consistent with reported values in northern peatlands, which range from ~2 to ~92 mg L^{-1} (Avagyan et al., 2016, 2014; Beer et al., 2008; Jessen et al., 2014; O'Donnell et al., 2016; Raudina et al., 2021, 2018, 2017; Ulanowski and Branfireun, 2013; Wickland et al., 2018a, 2007; Zhang et al., 2017). The higher DOC concentrations in the topsoil likely originate from plant root exudates and DOC production by

the enhanced microbial decomposition in warmer surface conditions (Borken et al., 2011; Hribljan et al., 2018; Kalbitz et al., 2000; Kang et al., 2001). Concentrations of DOC and DTN and their variation amplitudes decreased with depth likely due to limited SOM processing and DOC production, for example through phenol oxidase (Borken et al., 2011; Hribljan et al., 2018; Kane et al., 2010; Raudina et al., 2017). The reduced microbial activity in depth could originate from: 1) colder conditions (Davidson and Janssens, 2006), 2) lower nutrient availability limiting microbial (Avagyan et al., 2014; Kang et al., 2018; Sinsabaugh, 2010), and 3) anoxic conditions resulting from the waterlogged conditions lasting longer down the profile than at the surface (Beer et al., 2008; Fenner and Freeman, 2011; Hribljan et al., 2018).

Ratios of soil C/N and pore water DOC:TDN provide insights about the peat organic matter composition (Davidson and Janssens, 2006; Kalbitz et al., 2000). Greater soil C/N ratios in the topsoil than in the deeper layers may originate from preferential microbial degradation of N-rich organic compounds at the surface (Hobbie et al., 2002a; Hodgkins et al., 2014). The decrease of DOC/DTN ratios with depth suggests an early stage of dissolution of organic substrates at the base of the active layer, which thawed latter in the season compared to surface layers. Hydrophilic substances, which have lower C/N ratio, are preferentially released into soil solution and more prone to microbial decomposition (Kalbitz et al., 2000), as supported by higher DOC/DTN ratio in capillary (higher residence time) than in gravitational waters which illustrates dissolution of C-rich molecules. In addition, the thaw of the upper layers of the permafrost may release low aromatic nitrogen-rich DOM (Hodgkins et al., 2014; Lim et al., 2021; Schädel et al., 2014; Wickland et al., 2018a, 2007) and inorganic nitrogen such as ammonium previously stored frozen (Beermann et al., 2017; Elberling et al., 2010; Fouché et al., 2020; Keuper et al., 2012).

The low concentrations of the SO_4^{2-}, NO_3^-, K^+ and Na^+ of the Histic Cryosol pore water were consistent with the range of values for water in bogs (Andersen et al., 2011; Payette et al., 2001; Raudina et al., 2021, 2018, 2017; Ulanowski and Branfireun, 2013). Concentrations of Cl^-, Mg^{2+} and Ca^{2+} were closer to poorly mineralized fens (Avagyan et al., 2014; Hribljan et al., 2018; Payette et al., 2001). Major ions can be used as tracer of water sources along summer in peatlands (Avagyan et al., 2014; Bjorkman et al., 2018; Hribljan et al., 2018). The higher concentrations of Cl^- and Na^+ in soil solutions in surface horizons illustrate wet and dry atmospheric depositions and dilution with depth in the soil profile (Reeve et al., 1996). The increase in Mg^{2+} and Ca^{2+} concentrations with depth in the Histic Cryosol, associated with similar Ca/Na ratio as the upstream stream likely illustrates the inputs from mineral rich supra-permafrost groundwater flowing through the surrounding slopes, which also sustain the summer H stream discharge (Hribljan et al., 2018; Siegel et al., 1995; Ulanowski and Branfireun, 2013).

4.3. Increasing cation concentrations in deep horizons of the Turbic Cryosol active layer

The Turbic Cryosol pore water displayed pH, EC, DOC and TDN values similar to reported values in mineral soil layers (Deuerling et al., 2018; Drake et al., 2015; Jessen et al., 2014; Kokelj and Burn, 2005; Wickland et al., 2018b) with increasing total solute concentrations and decreasing DOC and DTN concentrations with depth. Major element concentrations of the Turbic Cryosol pore water lied within the few reported values available in permafrost environments (Jessen et al., 2014; Kokelj and Burn, 2005; Lamhonwah et al., 2017, 2016; Pokrovsky et al., 2006). Compared to mineral soils non affected by permafrost and located in different ecosystems, SO_4^{2-}, NO_3^- concentrations in the Turbic Cryosol pore waters were lower while Na^+ and Cl^- ranged within the reported values

(Lofgren et al., 2010; Manderscheid and Matzner, 1995; Schilli et al., 2010; Schlotter et al., 2012; Watmough et al., 2013).

As expected, DOC concentrations decreased with depth following the soil C content trend (Guigue et al., 2015) because of microbial uptake in surface horizons, organic compounds adsorptions onto mineral particles (Kalbitz et al., 2000; Moore, 2003) and dilution in the groundwater at depth (Borken et al., 2011). The important DOC content variations during the early stages of the growing season may result from snow melt and organic layer thaw (Kalbitz et al., 2000). Because water flows are impossible when the soil is frozen, dissolved organic matter has likely accumulated at soil surface and was leached downward when the snow melted and the ground thawed (Buckeridge et al., 2010; Larsen et al., 2002). DOC/DTN decreased with depth illustrating a change in the soil organic matter composition. The C/N ratio in mineral layers were typical of circumpolar mineral Cryosols (Schädel et al., 2014; Wickland et al., 2018b). Lower C/N and DOC/DTN ratios in mineral layers compare to organic top layers suggest lower contents of condensed aromatic organic compounds and a relative enrichment in N-rich plant organic compounds and microbial byproducts (Hodgkins et al., 2014; Kalbitz et al., 2000; Schädel et al., 2014). The decrease in DOC/DTN with depth may also reflect the preferential adsorption of more aromatic dissolved organic compounds onto mineral phases (Groeneveld et al., 2020) without the consumption of small plant-derived molecules by microorganisms at depth (Roth et al., 2019). DOC/DTN ratios of the soil solutions at 10 to 30 cm depth were higher than the C/N for corresponding soil layers, being similar to the soil C/N ratio of the organic horizon (2 cm), suggesting that the organic topsoil, which displays the greatest SOC content and C/N ratios, provides dissolved C-rich compounds in soil horizons deeper in the active layer.

At all sampling depths of the Turbic Cryosols, DTN contents showed peaks during mid-July. We assumed this sharp increase might originate from the thaw front deepening that could have released solutes from the upper layers of permafrost (Beermann et al., 2017; Fouché et al., 2020; Lamhonwah et al., 2016; Lewis et al., 2012b). As reported in similar environments, concentrations of NO_3^- were low owing to limited organic matter decomposition and strong competition for nitrates by plants and microorganisms (Chen et al., 2018; Gough et al., 2016; Sistla et al., 2012; Wild et al., 2013).

The decrease in Cl^- concentration and the constant concentration of Na+ with depth, associated with capillary pore water (long residence time) being depleted in Cl^- and Na^+ compared to gravitational water (short residence time) illustrate that Cl^- and a fraction of Na^+ come from atmospheric depositions and uphill surface runoff. Concentrations of Ca^{2+}, Mg^{2+} and K^+, which increased with depth and were higher in capillary than gravitational water, illustrate a different source compared with Cl^-. Our results clearly show that the four major cations were provided by weathering of post-glacial marine sediments composed of Na-feldspars, K-feldspars, chlorite (Mg^{2+}), amphiboles (Ca^{2+}, Na^+, Mg^{2+}), illite (K^+), muscovite (K^+), dolomite (Ca^{2+}, Mg^{2+}) and calcium carbonates (Ca^{2+}, Table1). The Ca/Na and Mg/Na ratios, which differed from rainfall, increased with depth in capillary pore water illustrating the supply of weathering products. The relative dominance of Ca^{2+} and Mg^{2+} compare to Na^+ illustrates the greater contribution of soluble Ca-rich and Mg-rich minerals such as calcite and dolomite, which could originate from cryogenic processes (Jessen et al., 2014; Kokelj and Burn, 2005; Lemieux et al., 2016). The freeze-out of ions with active layer freeze-up increases the saturation index for calcite and dolomite, ultimately leading to cryogenic carbonate precipitation (Jessen et al., 2014; Killawee et al., 1998; Papadimitriou et al., 2004). Then, the dissolu-

tion of cryogenic carbonates, releasing Ca^{2+} and Mg^{2+}, occurs with thaw front deepening and protons inputs from dissolved CO_2 and organic acids (Jessen et al., 2014).

As demonstrated by Lemieux et al. 2016, the permafrost pore water of the upper 1-2m thick ice-rich layers of the marine sediments display low concentrations of dissolved salts due to successive leaching of Na^+ (highly mobile) by groundwater flow. Similarly, lower concentrations of major cations in surface mineral layers originate from the successive summer leaching and progressive removal of soluble cations with time. The successive freeze-thaw cycles have lead to accumulation of cations at the base of the active layer and uppermost permafrost as solutes are excluded downwards during the fall freeze-up (French, 2007; Kokelj and Burn, 2005; Lim et al., 2021). This solute freeze-out enrichment is associated with ice accumulation (Kokelj and Burn, 2005; Lamhonwah et al., 2017, 2016), and can be 7.5 times greater in the upper part of the permafrost than in the active layer (Kokelj and Burn, 2005; Lamhonwah et al., 2017, 2016; Lim et al., 2021).

4.4. Thaw front deepening and supra-permafrost inputs control biogeochemical functioning of Cryosols

In the Histic Cryosols, EC, TDS, Mg/Na, Ca/Na and Cl/Na ratios increased with the thaw front depth in soil pore waters. Our results suggest a shift in solute inputs in the permafrost bog located in low-centered polygons. In addition to precipitation, two sources of water could provide solutes to the soil solution of the Histic Cryosol (Ulanowski and Branfireun, 2013): solute-rich ice from the transient layer beneath the active layer and supra-permafrost groundwater from surrounding hills that flows through polygons during summer (Cochand et al., 2019; Kokelj and Burn, 2005; Lim et al., 2021). Owing to vertical gradients of ion concentrations and the increase in EC and TDS with thaw front depth, we assumed that the transient layer thaw and groundwater inputs likely provided solutes to the soil profiles (Jessen et al., 2014; Tye and Heaton, 2007). Studies previously reported that permafrost thaw through active layer thickening and ground ice exposure lead to both water and solute inputs to the soil pore water (Lamhonwah et al., 2017; Stutter and Billett, 2003) and to the surface water bodies (Kokelj et al., 2013; Lamhonwah et al., 2016). Based on water chemistry, we assume that the hydrological functioning of the studied peatland may shift during during summer. At the beginning of the growing season, the shallow thickness of the soil profile does not allow for the groundwater to flow through the peatland polygons and solutes are only provided by precipitation (rainfall and snow melt). With thaw front deepening, polygons may connect to supra-permafrost groundwater originating from upstream slopes and the underlying solute-rich transient layer. We acknowledge that we did not assess the hydrological connectivity between the polygons and the surrounding slopes but the water distribution in the polygon landform strongly suggest the presence of a suprapermafrost groundwater connected to the surrounding slopes (Fig. S9). We hypothesize that the peatland shifted from a bog-like to a fen-like peatland during the growing season. In the context of warming-induced permafrost degradation, we hypothesize that the active layer thickening may change the nutrient availability of some permafrost affected peatlands, depending on the local conditions (active layer and peatland thickness, presence of active streams and groundwater) and microtopography (trough network, type of polygons), altering plant and microorganism communities (Bjorkman et al., 2018; Chen et al., 2018; Deslippe et al., 2005; Gough et al., 2016; Keuper et al., 2017; Mack et al., 2004).

At the Turbic site, EC, TDS and Ca^{2+}, Mg^{2+} and Na^+ concentrations increased with the thaw front deepening. These elements likely originate from the mineral phase dissolution (dolomite in

particular) and the transient layer thaw (Jessen et al., 2014; Kokelj and Burn, 2005; Lamhonwah et al., 2017, 2016). Indeed, in permafrost soils, the transient layer, which experiences freeze and thaw cycles at the decadal and centennial timescales (French and Shur, 2010; Shur et al., 2005), is characterized by high ice content and solute concentrations (Kokelj and Burn, 2005; Lamhonwah et al., 2017, 2016). Based on our observations, we assumed that permafrost degradation would enhance solute release from mineral permafrost soils to surface and subsurface waters.

In both soils, when winter comes and temperatures decrease, freezing fronts move downward and upward, and a new solute-rich frozen layer builds up from the solute-rich deep horizons of the active layer, which will further be available for mobilization with supra-permafrost water flow when the active layer thickness reaches again the transient layer in the subsequent years (Lamhonwah et al., 2016). While both soils display a similar enrichment in solute in depth and with thaw front deepening, changes in water stoichiometry along summer differ among soils. In the Turbic Cryosol, pore water stoichiometry did not evolve while it showed a enrichment in Ca^{2+} and Mg^{2+} in the Histic Cryosol with thaw front deepening. Changes in biogeochemical dynamics with climate-induced permafrost evolution will differ among Arctic watersheds depending on the contribution of the different permafrost soils in catchments, the landform properties and their hydrological connectivity to surface waters.

5. Conclusion

The parental material composition and various water sources controlled the chemistry of both capillary and gravitational waters. Both soils displayed low concentrations in nitrates. Gravitational and capillary water chemistry only differed in the Turbic Cryosol, the latter being enriched in DOC and cations while being less concentrated in anions than the former. We assumed that Cl^- was mainly provided by precipitation and sea sprays. On the other hand, cations were more concentrated in capillary than in gravitational waters originating from the weathering of soil silicate minerals and the ion-rich transient layer.

In both soils, concentrations of Ca^{2+} and Mg^{2+} increased with depth and their absolute concentrations as well as their relative abundance compared to Na^+ increased with thaw front and water table deepening. In the Turbic Cryosols, Mg^{2+} and Ca^{2+} concentrations were positively correlated with the thaw front and water table depths suggesting inputs from supra-permafrost groundwater draining the surrounding slopes and from the thaw of underlying solute-rich upper layers of the permafrost. In the Histic Cryosols, the seasonal thaw front and water table deepening contributes to the shift the peatland pore water chemistry due to inputs from supra-permafrost groundwater flows through surrounding slopes. We hypothesize that the studied permafrost bog undergoes a shift in its functioning from bog to fen during summer. We conclude that the diversity in natures and pedogenetic processes of permafrost soils should be considered to better understand the intra-watershed processes in the Arctic that affect further the global cycles. We also suggest that permafrost degradation may lead to an increase solute concentrations in soil pore waters in some locations depending on landscape settings.

Acknowledgments

This research is part of a PhD project that was funded by INSU, CNRS (grant n°19-2009-2012). Travels were helped by the PhD mobility grant from the Programme Frontenac funded by the “Fonds Québécois de Recherche sur la Nature et les Technologies” (FQRNT, grant n°163828). Fi-

nancial support was provided by CNRS INSU Chantier Arctique, the Arctic Net Network of Centers of Excellence, and the Arctic Development and Adaptation on Permafrost in Transition (ADAPT) program funded by the Natural Science and Engineering Research Council of Canada (NSERC). The authors want to thank the staff members of the Centre for Northern Studies (CEN) for essential help in northern logistics. Particular thanks to E. L'Hérault and D. Sarrazin for their field assistance. Finally, we gratefully acknowledge the northern community of Salluit for its hospitality and human support.

Data availability

The authors declare that all data supporting the findings of this study are available within the paper and its supplementary information. All data associated with this study are available from the corresponding author upon request and will shortly be posted on the Polar Data Catalogue metadata website (https://www.polardata.ca).

References

ACECSS, 1998. Agriculture Canadian Expert Committee on Soil Survey. The Canadian System of Soil Classification, Third Edition. ed. NRC - CNRC, Ottawa, Ontario.

Andersen, R., Rochefort, L., Landry, J., 2011. La chimie des tourbières du Québec : une synthèse de 30 années de données. Le naturaliste canadien 135, 5–14.

Avagyan, A., Runkle, B.R.K., Hartmann, J., Kutzbach, L., 2014. Spatial Variations in Pore-Water Biogeochemistry Greatly Exceed Temporal Changes During Baseflow Conditions in a Boreal River Valley Mire Complex, Northwest Russia. Wetlands 34, 1171–1182. https://doi.org/10.1007/s13157-014-0576-4

Avagyan, A., Runkle, B.R.K., Hennings, N., Haupt, H., Virtanen, T., Kutzbach, L., 2016. Dissolved organic matter dynamics during the spring snowmelt at a boreal river valley mire complex in Northwest Russia. Hydrol. Process. 30, 1727–1741. https://doi.org/10.1002/hyp.10710

Bagard, M.-L., Chabaux, F., Pokrovsky, O.S., Viers, J., Prokushkin, A.S., Stille, P., Rihs, S., Schmitt, A.-D., Dupr√©, B., 2011. Seasonal variability of element fluxes in two Central Siberian rivers draining high latitude permafrost dominated areas. Geochimica Et Cosmochimica Acta 75, 3335–3357.

Beel, C.R., Heslop, J.K., Orwin, J.F., Pope, M.A., Schevers, A.J., Hung, J.K.Y., Lafrenière, M.J., Lamoureux, S.F., 2021. Emerging dominance of summer rainfall driving High Arctic terrestrial-aquatic connectivity. Nature Communications 12, 1448. https://doi.org/10.1038/s41467-021-21759-3

Beer, J., Lee, K., Whiticar, M., Blodau, C., 2008. Geochemical controls on anaerobic organic matter decomposition in a northern peatland. Limnology and Oceanography 53, 1393–1407. https://doi.org/10.4319/lo.2008.53.4.1393

Beermann, F., Langer, M., Wetterich, S., Strauss, J., Boike, J., Fiencke, C., Schirrmeister, L., Pfeiffer, E.-M., Kutzbach, L., 2017. Permafrost Thaw and Liberation of Inorganic Nitrogen in Eastern Siberia. Permafrost and Periglacial Processes 28, 605–618. https://doi.org/10.1002/ppp.1958

Bintanja, R., Selten, F.M., 2014. Future increases in Arctic precipitation linked to local evaporation and sea-ice retreat. Nature 509, 479–482.

Biskaborn, B.K., Smith, S.L., Noetzli, J., Matthes, H., Vieira, G., Streletskiy, D.A., Schoeneich, P., Romanovsky, V.E., Lewkowicz, A.G., Abramov, A., Allard, M., Boike, J., Cable, W.L., Christiansen, H.H., Delaloye, R., Diekmann, B., Drozdov, D., Etzelmüller, B., Grosse, G.,

Guglielmin, M., Ingeman-Nielsen, T., Isaksen, K., Ishikawa, M., Johansson, M., Johannsson, H., Joo, A., Kaverin, D., Kholodov, A., Konstantinov, P., Kröger, T., Lambiel, C., Lanckman, J.-P., Luo, D., Malkova, G., Meiklejohn, I., Moskalenko, N., Oliva, M., Phillips, M., Ramos, M., Sannel, A.B.K., Sergeev, D., Seybold, C., Skryabin, P., Vasiliev, A., Wu, Q., Yoshikawa, K., Zheleznyak, M., Lantuit, H., 2019. Permafrost is warming at a global scale. Nature Communications 10, 264. https://doi.org/10.1038/s41467-018-08240-4

Bjorkman, A.D., Myers-Smith, I.H., Elmendorf, S.C., Normand, S., Rüger, N., Beck, P.S.A., Blach-Overgaard, A., Blok, D., Cornelissen, J.H.C., Forbes, B.C., Georges, D., Goetz, S.J., Guay, K.C., Henry, G.H.R., HilleRisLambers, J., Hollister, R.D., Karger, D.N., Kattge, J., Manning, P., Prevéy, J.S., Rixen, C., Schaepman-Strub, G., Thomas, H.J.D., Vellend, M., Wilmking, M., Wipf, S., Carbognani, M., Hermanutz, L., Lévesque, E., Molau, U., Petraglia, A., Soudzilovskaia, N.A., Spasojevic, M.J., Tomaselli, M., Vowles, T., Alatalo, J.M., Alexander, H.D., Anadon-Rosell, A., Angers-Blondin, S., Beest, M. te, Berner, L., Björk, R.G., Buchwal, A., Buras, A., Christie, K., Cooper, E.J., Dullinger, S., Elberling, B., Eskelinen, A., Frei, E.R., Grau, O., Grogan, P., Hallinger, M., Harper, K.A., Heijmans, M.M.P.D., Hudson, J., Hülber, K., Iturrate-Garcia, M., Iversen, C.M., Jaroszynska, F., Johnstone, J.F., Jørgensen, R.H., Kaarlejärvi, E., Klady, R., Kuleza, S., Kulonen, A., Lamarque, L.J., Lantz, T., Little, C.J., Speed, J.D.M., Michelsen, A., Milbau, A., Nabe-Nielsen, J., Nielsen, S.S., Ninot, J.M., Oberbauer, S.F., Olofsson, J., Onipchenko, V.G., Rumpf, S.B., Semenchuk, P., Shetti, R., Collier, L.S., Street, L.E., Suding, K.N., Tape, K.D., Trant, A., Treier, U.A., Tremblay, J.-P., Tremblay, M., Venn, S., Weijers, S., Zamin, T., Boulanger-Lapointe, N., Gould, W.A., Hik, D.S., Hofgaard, A., Jónsdóttir, I.S., Jorgenson, J., Klein, J., Magnusson, B., Tweedie, C., Wookey, P.A., Bahn, M., Blonder, B., Bodegom, P.M. van, Bond-Lamberty, B., Campetella, G., Cerabolini, B.E.L., Chapin, F.S., Cornwell, W.K., Craine, J., Dainese, M., Vries, F.T. de, Díaz, S., Enquist, B.J., Green, W., Milla, R., Niinemets, Ü., Onoda, Y., Ordoñez, J.C., Ozinga, W.A., Penuelas, J., Poorter, H., Poschlod, P., Reich, P.B., Sandel, B., Schamp, B., Sheremetev, S., Weiher, E., 2018. Plant functional trait change across a warming tundra biome. Nature 57–62. https://doi.org/10.1038/s41586-018-0563-7

Borken, W., Ahrens, B., Schulz, C., Zimmermann, L., 2011. Site-to-site variability and temporal trends of DOC concentrations and fluxes in temperate forest soils. Global Change Biology 17, 2428–2443.

Bouchard, F., Agnan, Y., Bröder, L., Fouché, J., Hirst, C., Sjöberg, Y., Team, the S., 2020. The SPLASH Action Group – Towards standardized sampling strategies in permafrost science. Adv. Polar Sci. 0–0. https://doi.org/10.13679/j.advps.2020.0009

Brennan, S.R., Fernandez, D.P., Mackey, G., Cerling, T.E., Bataille, C.P., Bowen, G.J., Wooller, M.J., 2014. Strontium isotope variation and carbonate versus silicate weathering in rivers from across Alaska: Implications for provenance studies. Chemical Geology 389, 167–181. https://doi.org/10.1016/j.chemgeo.2014.08.018

Buckeridge, K., Cen, Y.-P., Layzell, D., Grogan, P., 2010. Soil biogeochemistry during the early spring in low Arctic mesic tundra and the impacts of deepened snow and enhanced nitrogen availability. Biogeochemistry 99, 127–141.

Carey, S.K., 2003. Dissolved organic carbon fluxes in a discontinuous permafrost subarctic alpine catchment. Permafrost Periglac. Process. 14, 161–171. https://doi.org/10.1002/ppp.444

Chen, L., Liu, L., Mao, C., Qin, S., Wang, J., Liu, F., Blagodatsky, S., Yang, G., Zhang, Q., Zhang, D., Yu, J., Yang, Y., 2018. Nitrogen availability regulates topsoil carbon dynamics after permafrost thaw by altering microbial metabolic efficiency. Nature Communications 9, 3951. https://doi.org/10.1038/s41467-018-06232-y

Chu, H., Grogan, P., 2010. Soil microbial biomass, nutrient availability and nitrogen mineralization potential among vegetation-types in a low arctic tundra landscape. Plant and Soil 329, 411–420. https://doi.org/10.1007/s11104-009-0167-y

Cochand, M., Molson, J., Lemieux, J.-M., 2019. Groundwater hydrogeochemistry in permafrost regions. Permafrost and Periglacial Processes 30, 90–103. https://doi.org/10.1002/ppp.1998

Csank, A.Z., Czimczik, C.I., Xu, X., Welker, J.M., 2019. Seasonal Patterns of Riverine Carbon Sources and Export in NW Greenland. Journal of Geophysical Research: Biogeosciences 124, 840–856. https://doi.org/10.1029/2018JG004895

Darmody, R.G., Thorn, C.E., Harder, R.L., Schlyter, J.P.L., Dixon, J.C., 2000. Weathering implications of water chemistry in an Arctic-alpine environment, northern Sweden. Geomorphology 34, 89–100.

Davidson, E.A., Janssens, I.A., 2006. Temperature sensitivity of soil carbon decomposition and feedbacks to climate change. Nature 440, 165–173.

de Caritat, P., Hall, G., Gislason, S., Belsey, W., Braun, M., Goloubeva, N.I., Olsen, H.K., Scheie, J.O., Vaive, J.E., 2005. Chemical composition of Arctic snow: concentration levels and regional distribution of major elements. Science of The Total Environment 336, 183–199.

Deslippe, J.R., Egger, K.N., Henry, G.H.R., 2005. Impacts of warming and fertilization on nitrogen-fixing microbial communities in the Canadian High Arctic. FEMS Microbiol Ecol 53, 41–50. https://doi.org/10.1016/j.femsec.2004.12.002

Deuerling, K.M., Martin, J.B., Martin, E.E., Scribner, C.A., 2018. Hydrologic exchange and chemical weathering in a proglacial watershed near Kangerlussuaq, west Greenland. Journal of Hydrology 556, 220–232. https://doi.org/10.1016/j.jhydrol.2017.11.002

Douglas, T.A., Sturm, M., 2004. Arctic haze, mercury and the chemical composition of snow across northwestern Alaska. Atmospheric Environment 38, 805–820.

Drake, T., Tank, S.E., Zhulidov, A.V., Holmes, R.M., Gurtovaya, T.Yu., Spencer, R.G.M., 2018. Increasing Alkalinity Export from Large Russian Arctic Rivers. Environ. Sci. Technol. https://doi.org/10.1021/acs.est.8b01051

Drake, T.W., Wickland, K.P., Spencer, R.G.M., McKnight, D.M., Striegl, R.G., 2015. Ancient low-molecular-weight organic acids in permafrost fuel rapid carbon dioxide production upon thaw. Proceedings of the National Academy of Sciences 112, 13946–13951. https://doi.org/10.1073/pnas.1511705112

Edwards, K.A., McCulloch, J., Peter Kershaw, G., Jefferies, R.L., 2006. Soil microbial and nutrient dynamics in a wet Arctic sedge meadow in late winter and early spring. Soil Biology and Biochemistry 38, 2843–2851. http://dx.doi.org/10.1016/j.soilbio.2006.04.042

Elberling, B., Christiansen, H.H., Hansen, B.U., 2010. High nitrous oxide production from thawing permafrost. Nature Geoscience 3, 332–335. https://doi.org/10.1038/ngeo803

Elberling, B., Jakobsen, B.H., 2000. Soil solution pH measurements using in-line chambers with tension lysimeters. Can. J. Soil. Sci. 80, 283–288. https://doi.org/10.4141/S99-061

Fenner, N., Freeman, C., 2011. Drought-induced carbon loss in peatlands. Nature Geoscience 4, 895–900. https://doi.org/10.1038/ngeo1323

Fouché, J., Christiansen, C.T., Lafrenière, M.J., Grogan, P., Lamoureux, S.F., 2020. Canadian permafrost stores large pools of ammonium and optically distinct dissolved organic matter. Nature Communications 11, 4500. https://doi.org/10.1038/s41467-020-18331-w

Fouché, J., Keller, C., Allard, M., Ambrosi, J.P., 2017a. Diurnal evolution of the temperature sensitivity of CO2 efflux in permafrost soils under control and warm conditions. Science of The Total Environment 581–582, 161–173. https://doi.org/10.1016/j.scitotenv.2016.12.089

Fouché, J., Keller, C., Allard, M., Ambrosi, J.P., 2014. Increased CO2 fluxes under warming tests and soil solution chemistry in Histic and Turbic Cryosols, Salluit, Nunavik, Canada. Soil Biology and Biochemistry 68, 185–199. http://dx.doi.org/10.1016/j.soilbio.2013.10.007

Fouché, J., Lafrenière, M.J., Rutherford, K., Lamoureux, S., 2017b. Seasonal hydrology and permafrost disturbance impacts on dissolved organic matter composition in High Arctic headwater catchments. Arctic Science 3, 378–405. https://doi.org/10.1139/as-2016-0031

French, H., Shur, Y., 2010. The principles of cryostratigraphy. Earth-Science Reviews 101, 190–206. https://doi.org/10.1016/j.earscirev.2010.04.002

French, H.M., 2007. The Periglacial Environment 3rd edn. John Wiley.

Frey, K.E., McClelland, J.W., 2009. Impacts of permafrost degradation on Arctic river biogeochemistry. Hydrological Processes 23, 169–182.

Gagnon, S., Allard, M., 2020. Changes in ice-wedge activity over 25 years of climate change near Salluit, Nunavik (northern Québec, Canada). Permafrost and Periglacial Processes 31, 69–84. https://doi.org/10.1002/ppp.2030

Gaillardet, J., Dupré, B., Louvat, P., Allègre, C.J., 1999. Global silicate weathering and CO2 consumption rates deduced from the chemistry of large rivers. Chemical Geology 159, 3–30. https://doi.org/10.1016/S0009-2541(99)00031-5

Gough, L., Bettez, N.D., Slavik, K.A., Bowden, W.B., Giblin, A.E., Kling, G.W., Laundre, J.A., Shaver, G.R., 2016. Effects of long-term nutrient additions on Arctic tundra, stream, and lake ecosystems: beyond NPP. Oecologia 182, 653–665. https://doi.org/10.1007/s00442-016-3716-0

Groeneveld, M., Catalán, N., Attermeyer, K., Hawkes, J., Einarsdóttir, K., Kothawala, D., Bergquist, J., Tranvik, L., 2020. Selective Adsorption of Terrestrial Dissolved Organic Matter to Inorganic Surfaces Along a Boreal Inland Water Continuum. Journal of Geophysical Research: Biogeosciences 125, e2019JG005236. https://doi.org/10.1029/2019JG005236

Guigue, J., Lévêque, J., Mathieu, O., Schmitt-Kopplin, P., Lucio, M., Arrouays, D., Jolivet, C., Dequiedt, S., Chemidlin Prévost-Bouré, N., Ranjard, L., 2015. Water-extractable organic matter linked to soil physico-chemistry and microbiology at the regional scale. Soil Biology and Biochemistry 84, 158–167. https://doi.org/10.1016/j.soilbio.2015.02.016

Guo, L., Ping, C.-L., Macdonald, R.W., 2007. Mobilization pathways of organic carbon from permafrost to Arctic rivers in a changing climate. Geophysical Research Letters 34, L13603.

Harms, T.K., Abbott, B.W., Jones, J.B., 2014. Thermo-erosion gullies increase nitrogen available for hydrologic export. Biogeochemistry 117, 299–311. https://doi.org/10.1007/s10533-013-9862-0

Hobbie, S., Nadelhoffer, K., H√∂gberg, P., 2002a. A synthesis: The role of nutrients as constraints on carbon balances in boreal and arctic regions. Plant and Soil 242, 163–170. https://doi.org/10.1023/a:1019670731128

Hobbie, S., Nadelhoffer, K., H√∂gberg, P., 2002b. A synthesis: The role of nutrients as constraints on carbon balances in boreal and arctic regions. Plant and Soil 242, 163–170. https://doi.org/10.1023/a:1019670731128

Hodgkins, S.B., Tfaily, M.M., McCalley, C.K., Logan, T.A., Crill, P.M., Saleska, S.R., Rich, V.I., Chanton, J.P., 2014. Changes in peat chemistry associated with permafrost thaw increase greenhouse gas production. Proceedings of the National Academy of Sciences 111, 5819–5824. https://doi.org/10.1073/pnas.1314641111

Hribljan, J.A., Kane, E.S., Pypker, T.G., Chimner, R.A., 2018. The effect of long-term water table manipulations on dissolved organic carbon dynamics in a poor fen peatland. Journal of Geophysical Research: Biogeosciences 119, 577–595. https://doi.org/10.1002/2013JG002527

Hugelius, G., Strauss, J., Zubrzycki, S., Harden, J.W., Schuur, E.A.G., Ping, C.L., Schirrmeister, L., Grosse, G., Michaelson, G.J., Koven, C.D., O'Donnell, J.A., Elberling, B., Mishra, U., Camill, P., Yu, Z., Palmtag, J., Kuhry, P., 2014. Estimated stocks of circumpolar permafrost carbon with quantified uncertainty ranges and identified data gaps. Biogeosciences 11, 6573–6593. https://doi.org/10.5194/bg-11-6573-2014

Hughes-Allen, L., Bouchard, F., Laurion, I., Séjourné, A., Marlin, C., Hatté, C., Costard, F., Fedorov, A., Desyatkin, A., 2021. Seasonal patterns in greenhouse gas emissions from thermokarst lakes in Central Yakutia (Eastern Siberia). Limnology and Oceanography 66, S98–S116. https://doi.org/10.1002/lno.11665

Humborg, C., Blomqvist, S., Avsan, E., Bergensund, Y., Smedberg, E., Brink, J., M√∏rth, C.-M., 2002. Hydrological alterations with river damming in northern Sweden: Implications for weathering and river biogeochemistry. Global Biogeochemical Cycles 16, 12-1-12–13.

Iavorivska, L., Boyer, E.W., DeWalle, D.R., 2016. Atmospheric deposition of organic carbon via precipitation. Atmospheric Environment, Acid Rain and its Environmental Effects: Recent Scientific Advances 146, 153–163. https://doi.org/10.1016/j.atmosenv.2016.06.006

Jessen, S., Holmslykke, H.D., Rasmussen, K., Richardt, N., Holm, P.E., 2014. Hydrology and pore water chemistry in a permafrost wetland, Ilulissat, Greenland. Water Resour. Res. 50, 4760–4774. https://doi.org/10.1002/2013WR014376

Jolivel, M., Allard, M., 2013. Thermokarst and export of sediment and organic carbon in the Sheldrake River watershed, Nunavik, Canada. Journal of Geophysical Research: Earth Surface 118, 1729–1745. https://doi.org/10.1002/jgrf.20119

Jones, A., Stolbosky, V., Tarnocai, C., Broll, G., Spaargaren, O., and Montanarella, L., 2010. Soil atlas of the Northern Circumpolar Region. European Commission. Publications Office of the European Union.

Kalbitz, K., Solinger, S., Park, J.H., Michalzik, B., Matzner, E., 2000. Controls on the dynamics of dissolved organic matter in soils: A review. Soil Science 165, 277–304.

Kane, E.S., Turetsky, M.R., Harden, J.W., McGuire, A.D., Waddington, J.M., 2010. Seasonal ice and hydrologic controls on dissolved organic carbon and nitrogen concentrations in a boreal-rich fen. J. Geophys. Res. 115, G04012. https://doi.org/10.1029/2010JG001366

Kang, H., Freeman, C., W. Ashendon, T., 2001. Effects of elevated CO2 on fen peat biogeochemistry. Science of The Total Environment 279, 45–50. https://doi.org/10.1016/S0048-9697(01)00724-0

Kang, H., Kwon, M.J., Kim, S., Lee, S., Jones, T.G., Johncock, A.C., Haraguchi, A., Freeman, C., 2018. Biologically driven DOC release from peatlands during recovery from acidification. Nature Communications 9, 3807. https://doi.org/10.1038/s41467-018-06259-1

Kasper, J.N., Allard, M., 2001. Late-Holocene climatic changes as detected by the growth and decay of ice wedges on the southern shore of Hudson Strait, northern Quebec, Canada. Holocene 11, 563–577.

Keller, K., Blum, J.D., Kling, G.W., 2010. Stream geochemistry as an indicator of increasing permafrost thaw depth in an arctic watershed. Chemical Geology 273, 76–81. https://doi.org/10.1016/j.chemgeo.2010.02.013

Kendrick, M.R., Huryn, A.D., Bowden, W.B., Deegan, L.A., Findlay, R.H., Hershey, A.E., Peterson, B.J., Beneš, J.P., Schuett, E.B., 2018. Linking permafrost thaw to shifting biogeochemistry and food web resources in an arctic river. Global Change Biology 24, 5738–5750. https://doi.org/10.1111/gcb.14448

Keuper, F., Bodegom, P.M. van, Dorrepaal, E., Weedon, J.T., Hal, J. van, Logtestijn, R.S.P. van, Aerts, R., 2012. A frozen feast: thawing permafrost increases plant-available nitrogen in subarctic peatlands. Global Change Biology 18, 1998–2007. https://doi.org/10.1111/j.1365-2486.2012.02663.x

Keuper, F., Dorrepaal, E., Bodegom, P.M. van, Logtestijn, R. van, Venhuizen, G., Hal, J. van, Aerts, R., 2017. Experimentally increased nutrient availability at the permafrost thaw front selectively enhances biomass production of deep-rooting subarctic peatland species. Global Change Biology 23, 4257–4266. https://doi.org/10.1111/gcb.13804

Keuper, F., Wild, B., Kummu, M., Beer, C., Blume-Werry, G., Fontaine, S., Gavazov, K., Gentsch, N., Guggenberger, G., Hugelius, G., Jalava, M., Koven, C., Krab, E.J., Kuhry, P., Monteux, S., Richter, A., Shahzad, T., Weedon, J.T., Dorrepaal, E., 2020. Carbon loss from northern circumpolar permafrost soils amplified by rhizosphere priming. Nature Geoscience 1–6. https://doi.org/10.1038/s41561-020-0607-0

Killawee, J.A., Fairchild, I.J., Tison, J.-L., Janssens, L., Lorrain, R., 1998. Segregation of solutes and gases in experimental freezing of dilute solutions: implications for natural glacial systems. Geochimica et Cosmochimica Acta 62, 3637–3655. https://doi.org/10.1016/S0016-7037(98)00268-3

Kokelj, S.V., Burn, C.R., 2005. Geochemistry of the active layer and near-surface permafrost, Mackenzie delta region, Northwest Territories, Canada. Canadian Journal of Earth Sciences 42, 37–48.

Kokelj, S.V., Jorgenson, M.T., 2013. Advances in Thermokarst Research. Permafrost and Periglac. Process. 24, 108–119. https://doi.org/10.1002/ppp.1779

Kokelj, S.V., Kokoszka, J., van der Sluijs, J., Rudy, A.C.A., Tunnicliffe, J., Shakil, S., Tank, S., Zolkos, S., 2020. Permafrost thaw couples slopes with downstream systems and effects propagate through Arctic drainage networks. The Cryosphere Discussions 1–43. https://doi.org/10.5194/tc-2020-218

Kokelj, S.V., Lacelle, D., Lantz, T.C., Tunnicliffe, J., Malone, L., Clark, I.D., Chin, K.S., 2013. Thawing of massive ground ice in mega slumps drives increases in stream sediment and solute flux across a range of watershed scales. Journal of Geophysical Research: Earth Surface 118, 681–692. https://doi.org/10.1002/jgrf.20063

Kokelj, S.V., Smith, C.A.S., Burn, C.R., 2002. Physical and chemical characteristics of the active layer and permafrost, Herschel Island, western Arctic Coast, Canada. Permafrost and Periglacial Processes 13, 171–185.

Krnavek, L., Simpson, W.R., Carlson, D., Domine, F., Douglas, T.A., Sturm, M., 2012. The chemical composition of surface snow in the Arctic: Examining marine, terrestrial, and atmospheric influences. Atmospheric Environment 50, 349–359.

Lafrenière, M.J., Lamoureux, S.F., 2013. Thermal Perturbation and Rainfall Runoff have Greater Impact on Seasonal Solute Loads than Physical Disturbance of the Active Layer. Permafrost and Periglacial Processes 24, 241–251. https://doi.org/10.1002/ppp.1784

Lamhonwah, D., Lafrenière, M.J., Lamoureux, S.F., Wolfe, B.B., 2017. Evaluating the hydrological and hydrochemical responses of a High Arctic catchment during an exceptionally warm summer. Hydrological Processes 31, 2296–2313. https://doi.org/10.1002/hyp.11191

Lamhonwah, D., Lafrenière, M.J., Lamoureux, S.F., Wolfe, B.B., 2016. Multi-year impacts of permafrost disturbance and thermal perturbation on High Arctic stream chemistry. Arctic Science 3, 254–276. https://doi.org/10.1139/as-2016-0024

Larsen, K.S., Jonasson, S., Michelsen, A., 2002. Repeated freeze/thaw cycles and their effects on biological processes in two Arctic ecosystem types. Applied Soil Ecology 21, 187–195.

Lemieux, J.-M., Fortier, R., Talbot-Poulin, M.-C., Molson, J., Therrien, R., Ouellet, M., Banville, D., Cochand, M., Murray, R., 2016. Groundwater occurrence in cold environments: examples from Nunavik, Canada. Hydrogeol J 24, 1497–1513. https://doi.org/10.1007/s10040-016-1411-1

Lewis, T., Lafrenière, M.J., Lamoureux, S.F., 2012a. Hydrochemical and sedimentary responses of paired High Arctic watersheds to unusual climate and permafrost disturbance, Cape Bounty, Melville Island, Canada. Hydrological Processes 26, 2003–2018. https://doi.org/10.1002/hyp.8335

Lewis, T., Lafrenière, M.J., Lamoureux, S.F., 2012b. Hydrochemical and sedimentary responses of paired High Arctic watersheds to unusual climate and permafrost disturbance, Cape Bounty, Melville Island, Canada. Hydrological Processes 26, 2003–2018. https://doi.org/10.1002/hyp.8335

Lim, A.G., Loiko, S.V., Kuzmina, D.M., Krickov, I.V., Shirokova, L.S., Kulizhsky, S.P., Vorobyev, S.N., Pokrovsky, O.S., 2021. Dispersed ground ice of permafrost peatlands: Potential unaccounted carbon, nutrient and metal sources. Chemosphere 266, 128953. https://doi.org/10.1016/j.chemosphere.2020.128953

Lindgren, A., Hugelius, G., Kuhry, P., 2018. Extensive loss of past permafrost carbon but a net accumulation into present-day soils. Nature 1. https://doi.org/10.1038/s41586-018-0371-0

Lofgren, S., Gustafsson, J.P., Bringmark, L., 2010. Decreasing DOC trends in soil solution along the hillslopes at two IM sites in southern Sweden. Geochemical modeling of organic matter solubility during acidification recovery. Science of The Total Environment 409, 201–210.

Mack, M.C., Schuur, E.A.G., Bret-Harte, M.S., Shaver, G.R., Chapin, F.S., 2004. Ecosystem carbon storage in Arctic tundra reduced by long-term nutrient fertilization. Nature 431, 440–443.

MacLean, R., Oswood, M.W., Irons, J.G., McDowell, W.H., 1999. The effect of permafrost on stream biogeochemistry: A case study of two streams in the Alaskan (U.S.A.) taiga. Biogeochemistry 47, 239–267. https://doi.org/10.1007/BF00992909

Manderscheid, B., Matzner, E., 1995. Spatial and temporal variation of soil solution chemistry and ion fluxes through the soil in a mature Norway Spruce (Picea abies (L.) Karst.) stand. Biogeochemistry 30, 99–114.

Mann, P.J., Eglinton, T.I., McIntyre, C.P., Zimov, N., Davydova, A., Vonk, J.E., Holmes, R.M., Spencer, R.G.M., 2015. Utilization of ancient permafrost carbon in headwaters of Arctic fluvial networks. Nature Communications 6, 7856. https://doi.org/10.1038/ncomms8856

Marion, G.M., Henry, G.H.R., Freckman, D.W., Johnstone, J., Jones, G., Jones, M.H., Levesque, E., Molau, U., Molgaard, P., Parsons, A.N., Svoboda, J., Virginia, R.A., 1997. Open-top designs for manipulating field temperature in high-latitude ecosystems. Global Change Biology 3, 20–32.

McClelland, J.W., Déry, S.J., Peterson, B.J., Holmes, R.M., Wood, E.F., 2006. A pan-arctic evaluation of changes in river discharge during the latter half of the 20th century. Geophys. Res. Lett. 33, L06715. https://doi.org/10.1029/2006GL025753

McNamara, J.P., Kane, D.L., Hobbie, J.E., Kling, G.W., 2008. Hydrologic and biogeochemical controls on the spatial and temporal patterns of nitrogen and phosphorus in the Kuparul River, Arctic Alaska. Hydrological Processes 22, 3294–3309.

Moore, T.R., 2003. Dissolved organic carbon in a northern boreal landscape. Global Biogeochemical Cycles 17, 1109.

Neff, J.C., Hooper, D.U., 2002. Vegetation and climate controls on potential CO2, DOC and DON production in northern latitude soils. Global Change Biology 8, 872–884.

Négrel, P., Allègre, C.J., Dupré, B., Lewin, E., 1993. Erosion sources determined by inversion of major and trace element ratios and strontium isotopic ratios in river water: The Congo Basin case. Earth and Planetary Science Letters 120, 59–76. https://doi.org/10.1016/0012-821X(93)90023-3

Nieminen, T.M., Derome, K., Meesenburg, H., De Vos, B., 2013. Chapter 16 - Soil Solution: Sampling and Chemical Analyses, in: Developments in Environmental Science. Elsevier, pp. 301–315.

O'Donnell, J.A., Aiken, G.R., Butler, K.D., Guillemette, F., Podgorski, D.C., Spencer, R.G.M., 2016. DOM composition and transformation in boreal forest soils: The effects of temperature and organic-horizon decomposition state. Journal of Geophysical Research: Biogeosciences 121, 2727–2744. https://doi.org/10.1002/2016JG003431

Pan, Y., Wang, Yuesi, Xin, J., Tang, G., Song, T., Wang, Yinghong, Li, X., Wu, F., 2010. Study on dissolved organic carbon in precipitation in Northern China. Atmospheric Environment 44, 2350–2357. https://doi.org/10.1016/j.atmosenv.2010.03.033

Papadimitriou, S., Kennedy, H., Kattner, G., Dieckmann, G.S., Thomas, D.N., 2004. Experimental evidence for carbonate precipitation and CO2 degassing during sea ice formation. Geochimica et Cosmochimica Acta 68, 1749–1761. https://doi.org/10.1016/j.gca.2003.07.004

Parfitt, R.L., Percival, H.J., Dahlgren, R.A., Hill, L.F., 1997. Soil and solution chemistry under pasture and radiata pine in New Zealand. Plant and Soil 191, 279–290.

Pastor, A., Wu, N., Skovsholt, L.J., Riis, T., 2020. Biofilm Growth in Two Streams Draining Mountainous Permafrost Catchments in NE Greenland. Journal of Geophysical Research: Biogeosciences 125, e2019JG005557. https://doi.org/10.1029/2019JG005557

Payette, S., Rochefort, L., Arseneault, D., Bhiry, N., Bouchard, A., Campbell, D.R., Caron, J., Desrochers, A., 2001. Ecologie des tourbières du Québec-Labrador. Les Presses de l'Université Laval.

Peterson, B.J., Holmes, R.M., McClelland, J.W., Vörösmarty, C.J., Lammers, R.B., Shiklomanov, A.I., Shiklomanov, I.A., Rahmstorf, S., 2002. Increasing River Discharge to the Arctic Ocean. Science 298, 2171–2173. https://doi.org/10.1126/science.1077445

Petrone, K.C., Jones, J.B., Hinzman, L.D., Boone, R.D., 2006. Seasonal export of carbon, nitrogen, and major solutes from Alaskan catchments with discontinuous permafrost. Journal of Geophysical Research: Biogeosciences 111, G02020.

Picouet, C., Dupré, B., Orange, D., Valladon, M., 2002. Major and trace element geochemistry in the upper Niger river (Mali): physical and chemical weathering rates and CO2 consumption. Chemical Geology 185, 93–124. https://doi.org/10.1016/S0009-2541(01)00398-9

Ping, C.L., Jastrow, J.D., Jorgenson, M.T., Michaelson, G.J., Shur, Y.L., 2014. Permafrost soils and carbon cycling. SOIL Discuss. 1, 709–756. https://doi.org/10.5194/soild-1-709-2014

Pokrovsky, O.S., Schott, J., Dupr√©, B., 2006. Trace element fractionation and transport in boreal rivers and soil porewaters of permafrost-dominated basaltic terrain in Central Siberia. Geochimica Et Cosmochimica Acta 70, 3239–3260.

Pokrovsky, O.S., Schott, J., Kudryavtzev, D.I., Dupré, B., 2005. Basalt weathering in Central Siberia under permafrost conditions. Geochimica et Cosmochimica Acta 69, 5659–5680. https://doi.org/10.1016/j.gca.2005.07.018

Pokrovsky, O.S., Viers, J., Dupr√©, B., Chabaux, F., Gaillardet, J., Audry, S., Prokushkin, A.S., Shirokova, L.S., Kirpotin, S.N., Lapitsky, S.A., Shevchenko, V.P., 2012. Biogeochemistry of carbon, major and trace elements in watersheds of northern Eurasia drained to the Arctic Ocean: The change of fluxes, sources and mechanisms under the climate warming prospective. Comptes Rendus Geoscience 344, 663--677.

Prokushkin, A.S., Gavrilenko, I.V., Abaimov, A.P., Prokushkin, S.G., Samusenko, A.V., 2006. Dissolved Organic Carbon in Upland Forested Watersheds Underlain by Continuous Permafrost in Central Siberia. Mitig Adapt Strat Glob Change 11, 223–240. https://doi.org/10.1007/s11027-006-1022-6

Prokushkin, A.S., Gleixner, G., McDowell, W.H., Ruehlow, S., Schulze, E.-D., 2007. Source- and substrate-specific export of dissolved organic matter from permafrost-dominated forested watershed in central Siberia. Global Biogeochemical Cycles 21. https://doi.org/10.1029/2007GB002938

Prokushkin, A.S., Kajimoto, T., Prokushkin, S.G., McDowell, W.H., Abaimov, A.P., Matsuura, Y., 2005. Climatic factors influencing fluxes of dissolved organic carbon from the forest floor in a continuous-permafrost Siberian watershed. Can. J. For. Res. 35, 2130–2140. https://doi.org/10.1139/x05-150

R Core Team, R.F. for S.C., 2012. R: A Language and Environment for Statistical Computing.

Raudina, T.V., Loiko, S.V., Kuzmina, D.M., Shirokova, L.S., Kulizhskiy, S.P., Golovatskaya, E.A., Pokrovsky, O.S., 2021. Colloidal organic carbon and trace elements in peat porewaters across a permafrost gradient in Western Siberia. Geoderma 390, 114971. https://doi.org/10.1016/j.geoderma.2021.114971

Raudina, T.V., Loiko, S.V., Lim, A., Manasypov, R.M., Shirokova, L.S., Istigechev, G.I., Kuzmina, D.M., Kulizhsky, S.P., Vorobyev, S.N., Pokrovsky, O.S., 2018. Permafrost thaw and climate

warming may decrease the CO2, carbon, and metal concentration in peat soil waters of the Western Siberia Lowland. Science of The Total Environment 634, 1004–1023. https://doi.org/10.1016/j.scitotenv.2018.04.059

Raudina, T.V., Loiko, S.V., Lim, A.G., Krickov, I.V., Shirokova, L.S., Istigechev, G.I., Kuzmina, D.M., Kulizhsky, S.P., Vorobyev, S.N., Pokrovsky, O.S., 2017. Dissolved organic carbon and major and trace elements in peat porewater of sporadic, discontinuous, and continuous permafrost zones of western Siberia. Biogeosciences 14, 3561–3584. https://doi.org/10.5194/bg-14-3561-2017

Reeve, A.S., Siegel, D.I., Glaser, P.H., 1996. Geochemical controls on peatland pore water from the Hudson Bay Lowland: a multivariate statistical approach. Journal of Hydrology 181, 285–304.

Reimann, C., De Caritat, P., Halleraker, J.H., Volden, T., Ayas, M., Niskavaara, H., Chekushin, V.A., Pavlov, V.A., 1997. Rainwater composition in eight Arctic catchments in northern Europe (Finland, Norway and Russia). Atmospheric Environment 31, 159–170.

Reyes, F.R., Lougheed, V.L., 2015. Rapid Nutrient Release from Permafrost Thaw in Arctic Aquatic Ecosystems. Arctic, Antarctic, and Alpine Research 47, 35–48. https://doi.org/10.1657/aaar0013-099

Romanovsky, V.E., Smith, S.L., Christiansen, H.H., Shiklomanov, N.I., Streletskiy, D.A., Drozdov, D.S., Malkova, G.V., Oberman, N.G., Kholodov, A.L., Marchenko, S.S., 2015. Terrestrial permafrost [in 'state of the climate in 2014']. Bull. Am. Meteorol. Soc. 96.

Roth, V.-N., Lange, M., Simon, C., Hertkorn, N., Bucher, S., Goodall, T., Griffiths, R.I., Mellado-Vázquez, P.G., Mommer, L., Oram, N.J., Weigelt, A., Dittmar, T., Gleixner, G., 2019. Persistence of dissolved organic matter explained by molecular changes during its passage through soil. Nature Geoscience 12, 755–761. https://doi.org/10.1038/s41561-019-0417-4

Santos, P.S.M., Otero, M., Santos, E.B.H., Duarte, A.C., 2011. Chemical composition of rainwater at a coastal town on the southwest of Europe: What changes in 20 years? Science of The Total Environment 409, 3548–3553.

Schädel, C., Schuur, E.A.G., Bracho, R., Elberling, B., Knoblauch, C., Lee, H., Luo, Y., Shaver, G.R., Turetsky, M.R., 2014. Circumpolar assessment of permafrost C quality and its vulnerability over time using long-term incubation data. Global Change Biology 20, 641–652. https://doi.org/10.1111/gcb.12417

Schilli, C., Lischeid, G., Rinklebe, J., 2010. Which processes prevail?: Analyzing long-term soil solution monitoring data using nonlinear statistics. Geoderma 158, 412–420.

Schlotter, D., Schack-Kirchner, H., Hildebrand, E.E., von Wilpert, K., 2012. Equivalence or complementarity of soil-solution extraction methods. Journal of Plant Nutrition and Soil Science 175, 236–244.

Schmidt, I.K., Jonasson, S., Shaver, G.R., Michelsen, A., Nordin, A., 2002. Mineralization and distribution of nutrients in plants and microbes in four Arctic ecosystems: responses to warming. Plant and Soil 242, 93–106.

Shibata, H., Petrone, K.C., Hinzman, L.D., Boone, R.D., 2003. Effect of fire on dissolved organic carbon and inorganic solutes in spruce forest in the permafrost region of interior Alaska. Soil Science and Plant Nutrition 49, 25–29. https://doi.org/10.1080/00380768.2003.10409975

Shur, Y., Hinkel, K.M., Nelson, F.E., 2005. The transient layer: implications for geocryology and climate-change science. Permafrost and Periglacial Processes 16, 5–17. https://doi.org/10.1002/ppp.518

Siegel, D.I., Reeve, A.S., Glaser, P.H., Romanowicz, E.A., 1995. Climate-driven flushing of pore water in peatlands. Nature 374, 531–533. https://doi.org/10.1038/374531a0

Sinsabaugh, R.L., 2010. Phenol oxidase, peroxidase and organic matter dynamics of soil. Soil Biology and Biochemistry 42, 391–404. https://doi.org/10.1016/j.soilbio.2009.10.014

Sistla, S.A., Asao, S., Schimel, J.P., 2012. Detecting microbial N-limitation in tussock tundra soil: Implications for Arctic soil organic carbon cycling. Soil Biology and Biochemistry 55, 78–84. https://doi.org/10.1016/j.soilbio.2012.06.010

Sjöberg, Y., Jan, A., Painter, S.L., Coon, E.T., Carey, M.P., O'Donnell, J.A., Koch, J.C., 2021. Permafrost Promotes Shallow Groundwater Flow and Warmer Headwater Streams. Water Resources Research 57, e2020WR027463. https://doi.org/10.1029/2020WR027463

Smith, S.L., Romanovsky, V.E., Lewkowicz, A.G., Burn, C.R., Allard, M., Clow, G.D., Yoshikawa, K., Throop, J., 2010. Thermal State of Permafrost in North America: A Contribution to the International Polar Year. Permafrost and Periglacial Processes 21, 117–135.

Spencer, R.G.M., Aiken, G.R., Butler, K.D., Dornblaser, M.M., Striegl, R.G., Hernes, P.J., 2009. Utilizing chromophoric dissolved organic matter measurements to derive export and reactivity of dissolved organic carbon exported to the Arctic Ocean: A case study of the Yukon River, Alaska. Geophysical Research Letters 36, L06401. https://doi.org/10.1029/2008gl036831

Stutter, M.I., Billett, M.F., 2003. Biogeochemical controls on streamwater and soil solution chemistry in a High Arctic environment. Geoderma 113, 127–146. http://dx.doi.org/10.1016/S0016-7061(02)00335-X

Tank, S.E., Raymond, P.A., Striegl, R.G., McClelland, J.W., Holmes, R.M., Fiske, G.J., Peterson, B.J., 2012. A land-to-ocean perspective on the magnitude, source and implication of DIC flux from major Arctic rivers to the Arctic Ocean. Global Biogeochemical Cycles 26. https://doi.org/10.1029/2011GB004192

Tarnocai, C., Bockheim, J.G., 2011. Cryosolic soils of Canada: Genesis, distribution, and classification. Canadian Journal of Soil Science 91, 749–762.

Treat, C.C., Marushchak, M.E., Voigt, C., Zhang, Y., Tan, Z., Zhuang, Q., Virtanen, T.A., Räsänen, A., Biasi, C., Hugelius, G., Kaverin, D., Miller, P.A., Stendel, M., Romanovsky, V., Rivkin, F., Martikainen, P.J., Shurpali, N.J., 2018. Tundra landscape heterogeneity, not interannual variability, controls the decadal regional carbon balance in the Western Russian Arctic. Global Change Biology 0. https://doi.org/10.1111/gcb.14421

Turetsky, M.R., Abbott, B.W., Jones, M.C., Anthony, K.W., Olefeldt, D., Schuur, E.A.G., Grosse, G., Kuhry, P., Hugelius, G., Koven, C., Lawrence, D.M., Gibson, C., Sannel, A.B.K., McGuire, A.D., 2020. Carbon release through abrupt permafrost thaw. Nature Geoscience 13, 138–143. https://doi.org/10.1038/s41561-019-0526-0

Turetsky, M.R., Abbott, B.W., Jones, M.C., Anthony, K.W., Olefeldt, D., Schuur, E.A.G., Koven, C., McGuire, A.D., Grosse, G., Kuhry, P., Hugelius, G., Lawrence, D.M., Gibson, C., Sannel, A.B.K., 2019. Permafrost collapse is accelerating carbon release. Nature 569, 32–34. https://doi.org/10.1038/d41586-019-01313-4

Tye, A.M., Heaton, T.H.E., 2007. Chemical and isotopic characteristics of weathering and nitrogen release in non-glacial drainage waters on Arctic tundra. Geochimica et Cosmochimica Acta 71, 4188–4205. https://doi.org/10.1016/j.gca.2007.06.040

Ulanowski, T.A., Branfireun, B.A., 2013. Small-scale variability in peatland pore-water biogeochemistry, Hudson Bay Lowland, Canada. Science of The Total Environment 454–455, 211–218.

Vasander, H., Kettunen, A., 2006. Carbon in Boreal Peatlands, in: Wieder, R.K., Vitt, D.H. (Eds.), Boreal Peatland Ecosystems, Ecological Studies. Springer Berlin Heidelberg, Berlin, Heidelberg, pp. 165–194. https://doi.org/10.1007/978-3-540-31913-9_9

Vazquez, A., Costoya, M., Pena, R.M., Garcia, S., Herrero, C., 2003. A rainwater quality monitoring network: a preliminary study of the composition of rainwater in Galicia (NW Spain). Chemosphere 51, 375–386.

Viers, J., Dupré, B., Braun, J.-J., Deberdt, S., Angeletti, B., Ngoupayou, J.N., Michard, A., 2000. Major and trace element abundances, and strontium isotopes in the Nyong basin rivers (Cameroon): constraints on chemical weathering processes and elements transport mechanisms in humid tropical environments. Chemical Geology 169, 211–241. https://doi.org/10.1016/S0009-2541(00)00298-9

Vitt, D.H., 2006. Functional Characteristics and Indicators of Boreal Peatlands, in: Wieder, R.K., Vitt, D.H. (Eds.), Boreal Peatland Ecosystems, Ecological Studies. Springer Berlin Heidelberg, Berlin, Heidelberg, pp. 9–24. https://doi.org/10.1007/978-3-540-31913-9_2

Vonk, J.E., Tank, S.E., Walvoord, M.A., 2019. Integrating hydrology and biogeochemistry across frozen landscapes. Nat Commun 10, 1–4. https://doi.org/10.1038/s41467-019-13361-5

Watmough, S., Koseva, I., Landre, A., 2013. A Comparison of Tension and Zero-Tension Lysimeter and PRS Probes for Measuring Soil Water Chemistry in Sandy Boreal Soils in the Athabasca Oil Sands Region, Canada. Water, Air, and Soil Pollution 224, 1–13.

Wickland, K.P., Aiken, G.R., Butler, K., Dornblaser, M.M., Spencer, R.G.M., Striegl, R.G., 2012. Biodegradability of dissolved organic carbon in the Yukon River and its tributaries: Seasonality and importance of inorganic nitrogen. Global Biogeochemical Cycles 26, GB0E03. https://doi.org/10.1029/2012gb004342

Wickland, K.P., Neff, J.C., Aiken, G.R., 2007. Dissolved Organic Carbon in Alaskan Boreal Forest: Sources, Chemical Characteristics, and Biodegradability. Ecosystems 10, 1323–1340. https://doi.org/10.1007/s10021-007-9101-4

Wickland, K.P., Waldrop, M., Aiken, G.R., Koch, J.C., Jorgenson, T., Striegl, R.G., 2018a. Dissolved organic carbon and nitrogen release from boreal Holocene permafrost and seasonally frozen soils of Alaska. Environ. Res. Lett. https://doi.org/10.1088/1748-9326/aac4ad

Wickland, K.P., Waldrop, M.P., Aiken, G.R., Koch, J.C., Jorgenson, M.T., Striegl, R.G., 2018b. Dissolved organic carbon and nitrogen release from boreal Holocene permafrost and seasonally frozen soils of Alaska. Environ. Res. Lett. 13, 065011. https://doi.org/10.1088/1748-9326/aac4ad

Wild, B., Schnecker, J., Barta, J., Capek, P., Guggenberger, G., Hofhansl, F., Kaiser, C., Lashchinsky, N., Mikutta, R., Mooshammer, M., Santruckova, H., Shibistova, O., Urich, T., Zimov, S.A., Richter, A., 2013. Nitrogen dynamics in Turbic Cryosols from Siberia and Greenland. Soil Biology and Biochemistry 67, 85–93.

Willey, J.D., Kieber, R.J., Eyman, M.S., Avery, G.B., 2000. Rainwater dissolved organic carbon: Concentrations and global flux. Global Biogeochem. Cycles 14, 139–148. https://doi.org/10.1029/1999GB900036

Wologo, E., Shakil, S., Zolkos, S., Textor, S., Ewing, S., Klassen, J., Spencer, R.G.M., Podgorski, D.C., Tank, S.E., Baker, M.A., O'Donnell, J.A., Wickland, K.P., Foks, S.S.W., Zarnetske, J.P., Lee-Cullin, J., Liu, F., Yang, Y., Kortelainen, P., Kolehmainen, J., Dean, J.F., Vonk, J.E., Holmes, R.M., Pinay, G., Powell, M.M., Howe, J., Frei, R.J., Bratsman, S.P., Abbott, B.W., 2021. Stream Dissolved Organic Matter in Permafrost Regions Shows Surprising Compositional Similarities but Negative Priming and Nutrient Effects. Global Biogeochemical Cycles 35, e2020GB006719. https://doi.org/10.1029/2020GB006719

WRB, 2007. IUSS Working Group World Reference Base for Soil Resources 2006, first update 2007.

Zarnetske, J.P., Gooseff, M.N., Brosten, T.R., Bradford, J.H., McNamara, J.P., Bowden, W.B., 2007. Transient storage as a function of geomorphology, discharge, and permafrost active layer conditions in Arctic tundra streams. Water Resources Research 43. https://doi.org/10.1029/2005WR004816

Zhang, X., He, J., Zhang, J., Polyakov, I., Gerdes, R., Inoue, J., Wu, P., 2013. Enhanced poleward moisture transport and amplified northern high-latitude wetting trend. Nature Clim. Change 3, 47–51. http://www.nature.com/nclimate/journal/v3/n1/abs/nclimate1631.html#supplementary-information

Zhang, X., Hutchings, J.A., Bianchi, T.S., Liu, Y., Arellano, A.R., Schuur, E.A.G., 2017. Importance of lateral flux and its percolation depth on organic carbon export in Arctic tundra soil: Implications from a soil leaching experiment. Journal of Geophysical Research: Biogeosciences 122, 796–810. https://doi.org/10.1002/2016JG003754

Zolkos, S., Tank, S.E., Kokelj, S.V., 2018. Mineral Weathering and the Permafrost Carbon-Climate Feedback. Geophysical Research Letters 45, 9623–9632. https://doi.org/10.1029/2018GL078748